UNIVERSITAT
POLITÈCNICA
DE VALÈNCIA

ESCUELA TÉCNICA
SUPERIOR INGENIERÍA
INDUSTRIAL VALENCIA

INDUSTRIAL ENGINEERING MASTER THESIS

ANALYSIS OF VARIOUS PHYSICAL PHENOMENA, VARIABLES AND CORRELATIONS OF CRITICAL HEAT FLUX (CHF) IN TWO-PHASE FLOW AND IMPROVEMENT OF PREDICTION MODELS

AUTHOR: ADRIÁN ZARZUELA PULIDO

SUPERVISOR: RAFAEL MIRÓ HERRERO

SUPERVISOR: DR. RAFAEL MACIÁN-JUAN

Academic year: 2020-21

Abstract

The aim of this work is to analyze the literature for mechanistic models and/or various flows parameters that could be used as so-called features to improve the prediction and test them with some statistical techniques. The theory regarding the critical heat flux and the two-phase flow patterns has been introduced for a better understanding of the incoming study. After the introduction, the further analysis of some predictions methods of the flow pattern has been carried out. The methods implemented are the Hewitt and Roberts map and the Mishima and Ishii criteria. Once the determination of the flow pattern is done, the next task has been to prove the accuracy of one method of CHF prediction, the W-3 Correlation. Based on the achieved information, some interesting conclusions have been collected by the subsequent test for some regression models and its comparison with the correlation.

INDEX

Nomenclature

CHF	Critical Heat Flux
q''	Critical Heat Flux
v	Subscript. Vapor phase
l	Subscript. Liquid phase
g	Subscript. Gas phase
α	Void fraction
x, X	Quality
h	Enthalpy
H_{in}	Inlet enthalpy
$\dot{m}, G$	Mass flux
V, v	Velocity
w	Phase velocity
j, w_s	Superficial velocity
S	Slip ratio
ρ	Density
D_H	Hydraulic Diameter
D_{he}	Equivalent heated diameter
D_e	Equivalent diameter of flow channel
g	Gravity constant
σ	Surface tension
P	Pressure
T	Temperature

1. Introduction

1.1 Heat transfer

The heat transfer between systems is a process that happens continuously in the nature, but what really is interesting in engineering is how to take benefit of the heat transfer phenomena for practical applications. One of the examples related to the daily life is the heating and air conditioning to regulate the temperature of habited spaces. Another similar example is the refrigeration of food through the heat extraction from the place.

The application that is related to this work is the transfer of heat produced in power plants, where the quantity of energy is much greater. Energy from the primary source is converted to thermic energy that is extracted and feeds a turbine to convert the energy in electricity. The type of the primary energy depends on the power plant. In the thermal power plants, the energy released by the fossil fuels (oil, natural gas and coal) is used to produce heat.

Regarding the nuclear power plants, the energy is extracted from the nuclear fuel. A controlled nuclear chain reaction produces heat in a continuous way. This heat is extracted through the refrigerant fluid to carry the energy to the alternator and get electrical energy. Although the source of heat is different (nuclear reaction vs combustion) the thermodynamic cycle of the nuclear plants is similar to the one of the conventional power plants. The extraction of heat may work properly; otherwise, the rise of temperature may produce significant damage in the facilities. Therefore, the real importance of the flow that extract the heat from the nuclear reaction. In order to control the heat extraction it is mandatory to know or predict the Critical Heat Flux that reduces the heat transfer coefficient. Nuclear reactor is a so called fixed heat flux type machine. If, for some reason, there is a decrease in the value of the heat transfer coefficient, the flow will be not able to extract all the heat produced, so the temperature will increase. This uncontrolled temperature increase (caused by the inability of the fluid to draw all the heat energy) can lead to accident conditions in nuclear power plants. That is why modeling the behavior of the refrigerant fluid through the pipe is essential in the nuclear industry. At these levels, where high power is handled, it is common to work with fluid flows that are in two phases. The relevance of the research of this type of flow remains not only in the study of the normal operation conditions but also in the accident conditions. This flow is extremely complex and the modeling is very difficult to perform in some situation (practically impossible to achieve (quasi)perfect models).

Attempts to predict the interactions between phases and most commonly used models to calculated the regimes in which the flow works are collected in the following work.

1.2 Two phase flow

The multiphase flow is defined by the existence of two or more separate phases in the flow. Although in the multiphase flow there are flows composed of more than two-phases, most of the applications that involve the handling of the multiphase flow work with two-phase flow, specifically with two-phase flows composed of one liquid phase and another gas phase. Boiling heat transfer phenomena are much

more complex than convection heat transfer, which is the method of heat transfer that happens when there is no phase change. In liquid phase convection, heat transfer can be described in general, in terms of geometry, density, coolant expansion coefficient, viscosity and thermal conduction. However, for boiling heat transfer, there are added complications (due to the different boiling patterns) such as surface conditions, heat flow or superficial tension, among others [2].

From an engineering point of view, the main objective of studying the two-phase flow is to determine the heat transfer and pressure variations of the flow [2]. The two-phase flow that implies changes between the liquid and gas phase is really important for the study of the heat transfer. Each phase has its own properties (temperature, density, speed ...). Through parameters such as the void fraction or the quality, the "participation" of each phase in the total flow can be defined. These parameters are variable, for example, the void fraction changes when evaporation occurs. Therefore, in many industrial applications it is necessary to consider a variable void fraction.

In order to define completely the two-phase flow composed of the liquid and gas phases in a pipe it is necessary to determine the flow pattern that describes the interaction and the way in which the two-phases are set in the flow. Flow patterns determine the distribution of phases and their characteristics, that is, they define the internal structures of the flow. The heat transfer coefficient is highly affected by the existing flow pattern in the pipe. It is important to predict adequately the flow pattern, in order to define the design and operation conditions and not endanger the safety of the installation. It is also important to note that the determination of the flow pattern is complex; it is not known exactly when a flow changes its flow pattern. The transition between flow patterns is carried out continuously with transition patterns, and there is no exact point from which a sudden transition occurs. It is because of its complexity, that there is no precise model to predict all the characteristics of the two-phase flow. Many determination methods of the flow pattern are based on empirical methods or approximate maps based on the flow characteristics. Even single-phase flows are complex systems due to the existence of turbulences. It could be said that knowing the flow pattern in a two-phase flow is the same as knowing when a flow is laminar or turbulent in a single-phase flow [3].

For applications of the two-phase vapor-liquid flow, it is pretended to have the control of the heat transfer that occurs in the flow. Moreover, since the flow patterns have a great impact on heat transfer, it is necessary to have a control of the patterns and evaluate which pattern is suitable in each application. If the temperature of the surface in contact with the flow is gradually increased (more precisely the excess temperature, which refers to the temperature difference between the surface temperature and the saturation temperature), the heat transfer will increase until certain point (called Critical Heat Flux) where an increase of the temperature does not imply an increase in heat transfer, but just the opposite.

1.3   Useful parameters of the two-phase flow

   a)   **Mass flux.** Quantity of mass that flows in a given area and time (Kg/m^2s).

b) **Pressure.** Force per unit of area exerted by the fluid (MPa). It is a measure of the potential energy contained in the fluid.

c) **Void fraction.** It is one of the most important parameters to characterize the two-phase flow and represents the relative quantity of each phase. It is a geometrical parameter that can be defined as the area occupied by gas phase in a section of the pipe:

$$\alpha \equiv \frac{A_v}{A_v + A_l} \tag{1}$$

The characteristics of the two-phases (density, heat transfer coefficient...) are very different, and that is why this parameter is that important. Obviously, the range of values between which the void fraction moves ranges from zero to one.

d) **Flow quality.** Quality refers to the mass fraction of vapor in the flow, therefore, its value is equal to one when the flow is saturated vapor and equal to zero when the flow is saturated liquid. The flow quality is defined as:

$$x \equiv \frac{\dot{m}_v}{\dot{m}_v + \dot{m}_l} \tag{2}$$

The quality can be negative when a subcooling condition occurs, which means that the temperature of the fluid is lower than the saturation temperature. With enough heat flux, bubbles can be created, even if the mean temperature of the fluid has not reached the saturation temperature. The equation related to negatives values of quality in the subcooling zone is the following [13]:

$$x = \frac{h_f - h_{f,sat}}{h_{g,sat} - h_{f,sat}} = -\frac{c_f \Delta T_{sub}}{h_{g,sat} - h_{f,sat}} \tag{3}$$

e) **Slip ratio.** It is defined as the ratio of the velocity of the vapor phase to the velocity of the liquid phase. In many two-phase flows, the velocity of the gas phase is significantly different from the velocity of the liquid phase [17].

$$S \equiv \frac{v_v}{v_l} = \frac{\rho_l x (1 - \alpha)}{\rho_v \alpha (1 - x)} \qquad (4)$$

The relationship between quality, void fraction and slip ratio is as follows:

$$S = \frac{1 - \alpha}{\alpha} \frac{x}{1 - x} \frac{\rho_l}{\rho_g} \qquad (5)$$
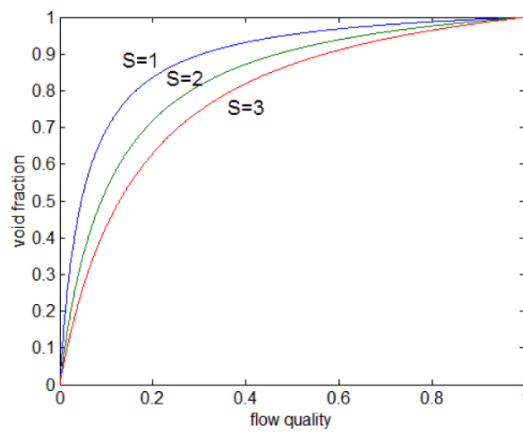
Figure 1. Flow quality vs void fraction for different slip ratios (water, pressure = 7 MPa). Source: MIT department of Nuclear Science and Engineering [17]

f) **Superficial velocity.** It is the velocity of the phase if the phase occupies the entire area of the pipe. Is defined as:

$$j_{phase} = \frac{G_{phase}}{\rho_{phase} A} \qquad (6)$$

Velocity of the phase and superficial velocity are related by the void fraction. The real velocity of the phase is defined as:

$$v_{phase} = \frac{j_{phase}}{\alpha_{phase}} \qquad (7)$$

g) **Mixture density.** Calculated through the void fraction:

$$\rho_{mixture} = \alpha\rho_v + (1-\alpha)\rho_l \qquad (8)$$

h) **Surface tension.** Important parameter for the stability between phases and the flow pattern. It controls the beginning of bubble growth after nucleation. The growth rate is low at first, but increases with the bubble size (the effect of superficial tension becomes less and less significant) [2].

i) **Viscosity.** It affects the hydrodynamic characteristics of the flow. An increase of the viscosity increases the coalescence rate of the bubbles and reduces the breaking rate [2].

j) **Diameter.** The hydraulic diameter commonly used for non-circular section tubes:

$$D_H = \frac{4A}{P_{wetted}} \qquad (9)$$

The equivalent heated diameter:

$$D_{he} = \frac{4A}{P_{heated}} \qquad (10)$$

1.4   Two-phase flow patterns and heat transfer regions

Flow patterns depend on the conditions of pressure, flow, heat transfer and pipe geometry. Depending on the flow pattern, there are different effects on the hydrodynamic conditions of the heated surface, and in this way, different pressure drops and different modes of heat transfer occur. The heat transfer regions and the flow patterns are completely related, therefore, the change in one implies the corresponding change in the other one.

Flow patterns are different depending on the orientation of the pipe and the direction of the flow. This is due to the action of gravitational and inertial forces, which act differently according to the orientation of the pipe, and the direction in which the fluid flow [21]. Therefore, an upward flow of the fluid in a vertical pipe will be considered to describe the theoretical behavior of the fluid.

The evolution followed by the fluid as the surface temperature of the pipe increases is described below and it is showed in the Figure 2. First, the fluid is in a single liquid phase, and the fluid satisfactorily extracts the energy by convection.

By increasing the heat transferred by the surface of the pipe to the fluid, there comes a time when the convection method is not strong enough, and the temperature of the wall overtakes the saturation temperature of the fluid. This new temperature of the pipe wall heats the liquid to the point of activating the nucleation. Bubbles begin to be generated on the surface, the boiling phenomenon remains and the presence of subcooled liquid appears. In this first stage, called partial nucleate boiling, convection is sustained in the central region of the pipe, while in areas of the surface the creation of small bubbles occurs. This heat transfer zone is called subcooled boiling, since boiling in the fluid is generated in the hot zone (in contact with the surface) even though the average temperature of the fluid is below the saturation temperature. When the liquid is in a subcooled state, the flow quality is considered to be negative. In the region where the liquid is subcooled, the flow pattern that is assumed to happen is the bubbly.

As the temperature of the walls increases even more, the areas where the phenomenon of boiling and bubble creation occurs considerably increases, to a point where the fully nucleate boiling is reached. Now, the entire surface of the pipe is in a state of nucleation. During saturated nucleation, heat transfer is affected by pressure and temperature, but not by flow velocity [2]. In this heat transfer region where the nucleate boiling is saturated, the present flow patterns may be Bubbly, Slug and Annular.

Flow nucleate boiling is characterized by having a very high heat transfer coefficient due to the formation of small bubbles on the surface. These bubbles separate from the surface and collapse due to the temperature of the fluid, thus the bubbles transport the heat to the main flow. It is due to its high heat transfer coefficient that nucleate boiling is used in a large number of heat exchangers in the industry or for the transport and extraction of energy, for example, in nuclear reactors.

In the flow nucleate boiling, the following mechanisms of energy transfer between the surface and the fluid are present. The transport of heat by the latent heat of the bubbles, related to the phase change of the liquid, and not with its change in temperature. Heat transport by micro layer evaporation and heat transfer by micro convection (at bubble level), and finally, heat transfer by single-phase convection between bubble zones. The real complexity lies in determining the participation of each mechanism in the total heat transfer for different nucleate flow boiling regimes [2].
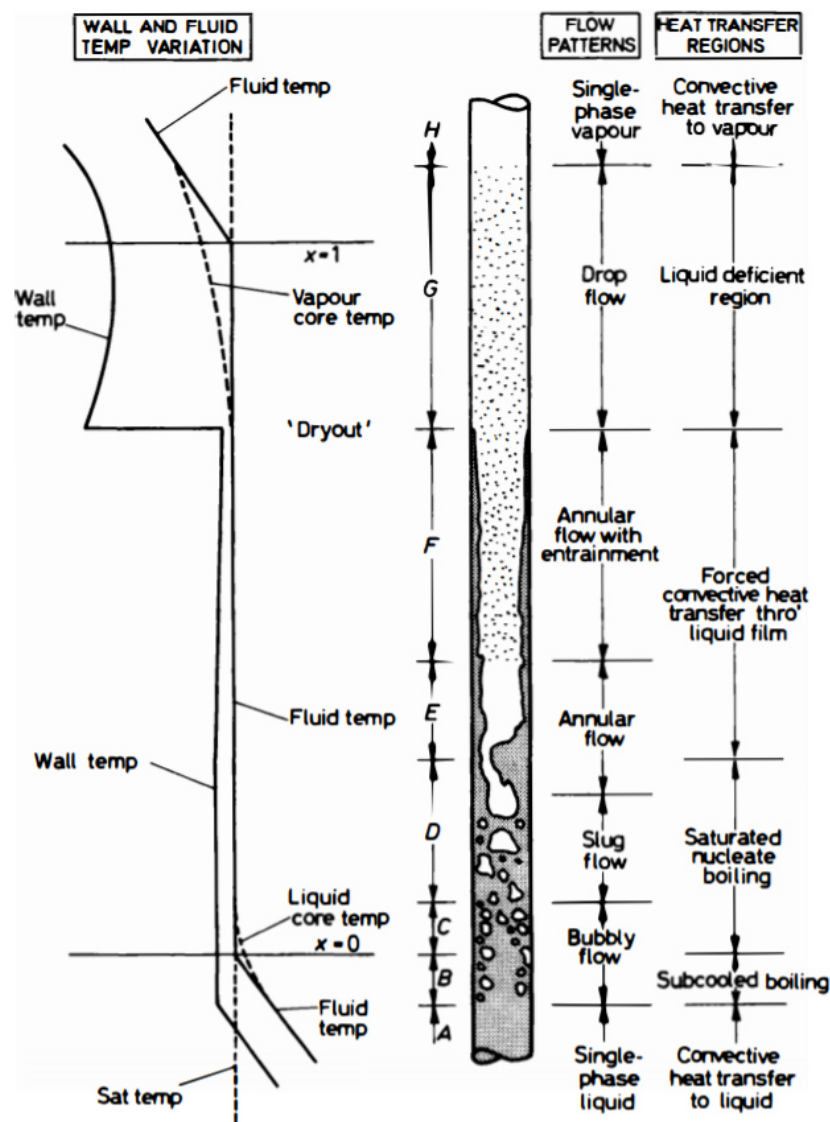
Figure 2. Regions of heat transfer in convective boiling. Source: Boiling Heat Transfer and Two-Phase flow. L.S Tong and Y. S.Tang

Once the complete nucleate boiling has been reached and all surface areas are in a nucleation state, if heat transfer is further increased, the critical heat flux is reached (B, Figure 3). From this point, there is a decrease in heat transfer, and a transition region begins. The boiling film zone is not yet reached. This area is called transition boiling. In this area, the heat transfer decreases as the surface temperature increases since the heat transfer mechanisms that are present are different from those of the previous mentioned regions. The heat transfer coefficient decreases until reaching the point of Leidenfrost (C, Figure 3).

The Leidenfrost effect is a physical phenomenon in which a vapor / gas layer in the area near the hot surface is produced. The vapor layer has a lower heat transfer coefficient and prevents the rest of the fluid from quickly evaporation.

The transition stage occurs gradually until stable film boiling, as the surface temperature rises above the Leidenfrost point. Then, if the temperature keeps increasing, the heat transfer coefficient gradually rises again in the boiling film stage.

This way, the critical heat flux can be described as the high heat transfer limit value related to the nucleate boiling, from which a vapor layer is produced (which has a worse heat transfer capacity) and thus deteriorates the heat transfer coefficient. From the CHF value, changes in the form of boiling appear. This form is associated with the term boiling crisis, essentially caused by a lack of coolant liquid in contact with the heat-transmitting surface.
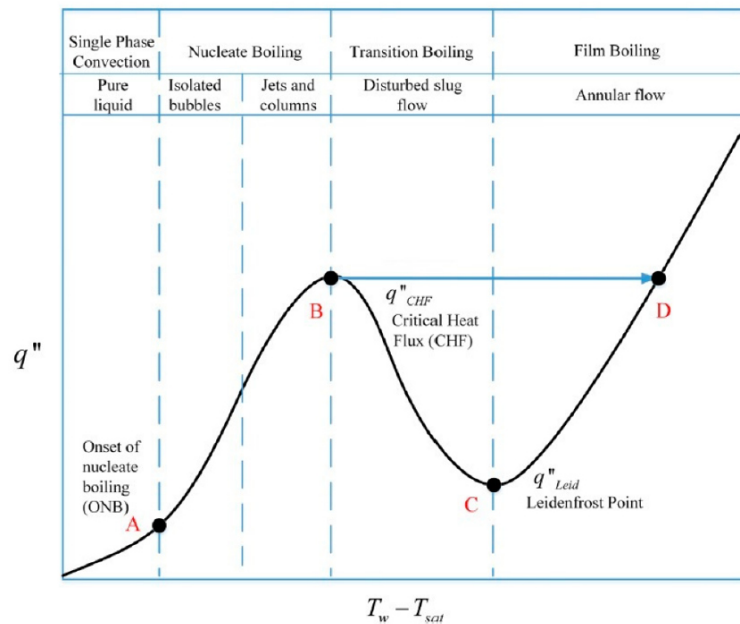
Figure 3. Boiling curve for water at atmospheric pressure. Source: "Boiling and Quenching Heat Transfer Advancement by Nanoscale Surface Modification." Hu, Hong.

Thus, the heat transfer regimes that occur when increasing the temperature of the surface are the convection (when the pure liquid is the present), the nucleate boiling, the film boiling and the transition zones that exist between all of them. The Figure 4 shows how these mechanisms are developed near the wall.
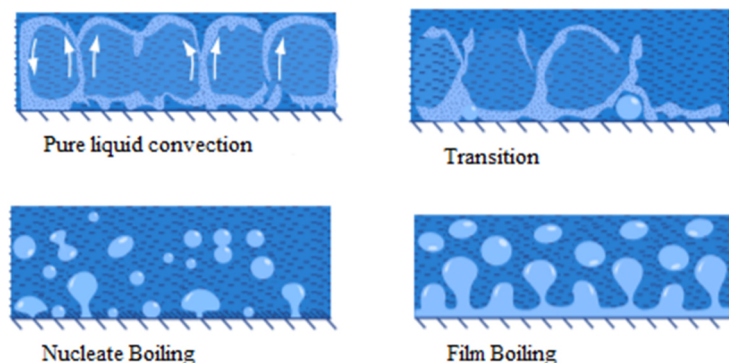
Figure 4. Heat transfer regimes in pool boiling. Source: MIT OpenCourseWare

1.4.1 Boiling crisis type

Boiling crisis can occur in different flow patterns. If the boiling crisis occurs in a bubbly flow, it is usually called departure from nucleate boiling (DNB). Nevertheless, if the boiling crisis occurs in an annular flow, it is usually called dry out. Therefore, the boiling crisis can be classified as dryout (which occurs in the high quality region) or departure from nucleate boiling (occurs in the subcooled or low quality region).

There is no exact value for which one phenomenon or another occurs. In short, beyond setting a limit specific value, the lower the flow quality, the greater the possibility of DNB being produced, and the higher the quality, the more likely that dryout will occur.

a) **Subcooled or low-quality region (boiling crisis).** It occurs at high heat transfer, which causes nucleate boiling. In subcooled bubbly flow, a layer of bubbles usually covers the surface where nucleate boiling occurs. There comes a time when the increase in the thickness of the bubble layer causes the overheating of the surface, giving rise to the boiling crisis. During the boiling crisis, the nucleate boiling disappears due to the spread of the local void as a vapor layer, and it is replaced by boiling film. The thickness of the bubble layer indicates the approximation to the DNB, and therefore the bubbly flow can be related to DNB and boiling crisis. Boiling crisis mechanisms in this region are characterized by the subcooling degree. At high subcooling, the overheating of the surface is caused by a low heat transfer capacity of the liquid core. At medium-low (bubbly) flow, DNB is produced by the agglomeration of bubbles and the creation of a vapor layer near the wall. At low quality flow, DNB is produced by the bursting of the bubbles under the liquid layer, in contact with the surface. These events are showed in the Figure 5 [2].
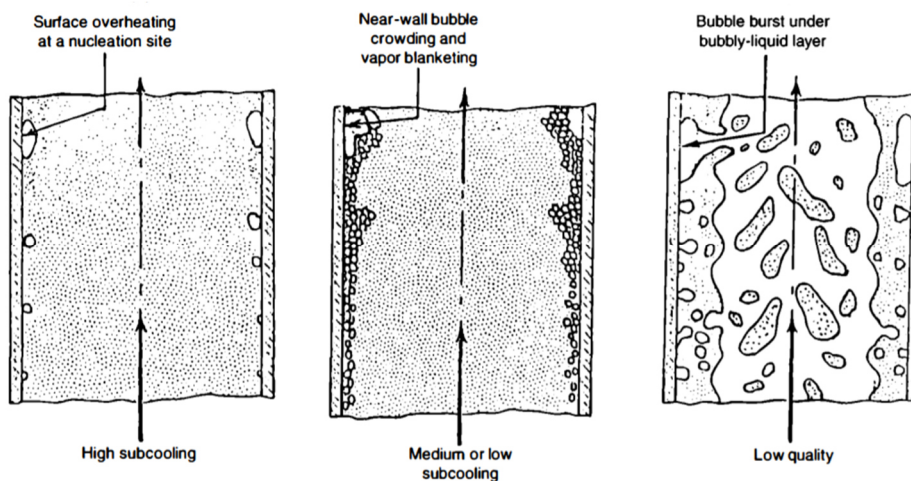
Figure 5. Mechanism of DNB in bubbly flows. Source: "Boiling heat transfer and two-phase flow". L.S. Tong and T.S. Tang

b) **High quality region (boiling crisis).** It occurs at a lower heat transfer level. In annular flow, which is generally the flow pattern at which this type of boiling crisis occurs, a layer of liquid covers the hot surface and acts as a coolant. In this case, the thinness of the liquid layer indicates the approach to dryout and the boiling crisis. If there is an excessive evaporation of the liquid layer, this layer breaks and the surface becomes dry. The critical heat flux (CHF) depends on the flow pattern parameters (flow quality, void fraction, velocity of the phases ...) and the liquid layer attached to the surface. Boiling crisis mechanisms in this region are characterized according to the value of quality. At medium quality annular flow, the dryout is produced by the interruption of the layer of the liquid phase caused by the instability of the surface waves. At high quality annular flow, the dryout is produced by drying the layer of the liquid phase on the hot surface. The difference between the high quality annular flow and medium quality annular flow is showed in the Figure 6 [2].
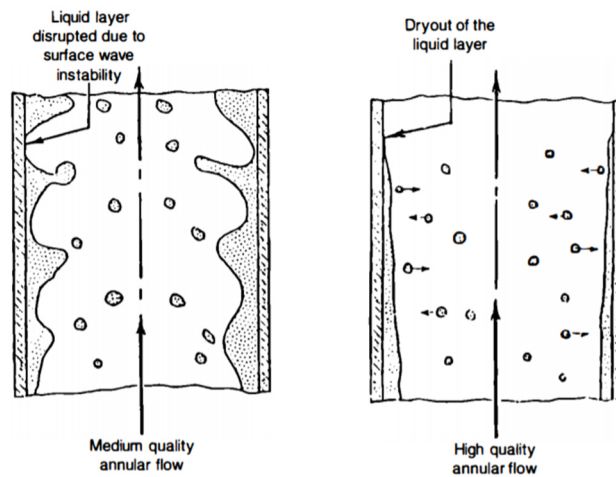
Figure 6. Mechanism of dryout in annular flows. Source: "Boiling heat transfer and two-phase flow". L.S. Tong and T.S. Tang

The behavior of the bubble layer (DNB) and the layer of liquid (Dryout) is an indicator of the approach to the CHF and therefore to the boiling crisis. The Figure 7 shows the comparison between the two boiling crisis mechanisms.
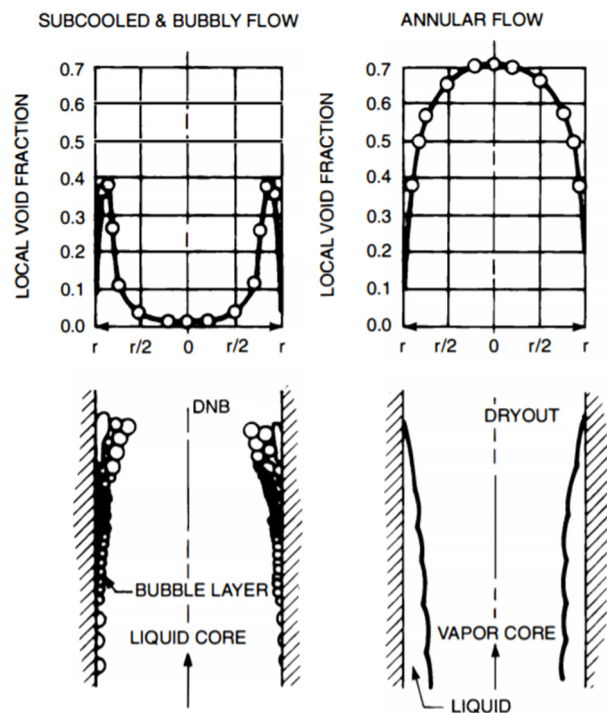
Figure 7. Comparison of boiling-crisis mechanism in various flow patterns. Source: "Boiling heat transfer and two-phase flow". L.S. Tong and T.S. Tang

When the CHF value is reached and the boiling crisis occurs, the surface temperature rises, since the heat cannot be eliminated quickly enough. This temperature increase of the surface is lower after the dryout phenomenon, compared to the subcooled boiling crisis.

It is so important to know the nature of the boiling crisis, since in the case of nuclear reactors design, the decrease of the heat transfer can lead to an inadmissible overheating that could damage the core. As it has been pointed out before, the nature of the boiling crisis is affected by the flow pattern of the flow, and therefore, it is necessary to distinguish the different patterns that can exist in the pipe. It should be noted that the flow patterns are in complete relationship with the different heat transfer zones.

Therefore, the difference in the heat transfer methods and the transfer between phases in the different flow patterns leads us to use criteria for determining flow patterns and correlations dependent on these flow patterns.

1.4.2 Flow patterns for vertical flow

The types of flow that may occur in vertical pipes are the following [3]:

a) **Bubbly.** The vapor phase is distributed in form of discrete bubbles within the continuous liquid phase. The bubbles are generally small and spherical. This flow pattern occurs at low void fractions. In turn, this type of pattern can be divided in different types depending on the behavior and interaction of the bubbles.

b) **Slug.** In this pattern the gas bubbles have approximately the diameter of the pipe. The nose of the bubble has a characteristic spherical shape and the gas in the bubble is separated from the wall by a layer of liquid. Between the large bubbles there are small bubbles that are detached from the wake of the large bubble. Gas distribution is due to the action of gravity. This flow occurs at moderate levels of void fraction and low flow rates.

c) **Churn.** Also known as semi-annular or slug-annular. It is formed by the breakage of the large characterized bubbles that come from the slug flow. The liquid is mainly found in the channel wall while the gas or vapor moves chaotically. This flow pattern has an oscillatory character over time. The bubbles become unstable when the velocity of the gas phase is increased.

d) **Wispy-annular.** The distribution of this pattern consists of a liquid layer region that moves slowly in the pipe walls while the rest of the liquid phase fraction is transported in the central gas core. The gas phase moves relatively faster. The liquid in the wall layer contains small gas bubbles inside, and the liquid phase carried in the gas core is found as large drops that have been grouped into long irregular filaments. This regime is characteristic for high mass velocities.

e) **Annular.** A liquid film is formed on the pipe wall with a central continuous flow of gas or vapor. Large waves appear on the surface of the liquid layer and its breaking is a source to the drop drag that occurs in the central gas core. The liquid drops are separated, unlike the wispy-annular flow pattern, where they are all agglomerated. This pattern occurs at high values of the void fraction and the flow velocity. The annular flow occurs in many industry applications, such as vapor generators, condensers or BWR nuclear reactors.

f) **Mist flow.** It occurs at high flow rates and high flow quality. These conditions cause the destruction of the liquid layer attached to the surface. The liquid phase is transported as small droplets into the gas phase.

Quality	Rate	Pattern
Low	Low	Bubbly
	Middle	Bubbly
	High	Dispersed bubbly
Middle	Low	Slug
	Middle	Slug
	High	Churn
High	High	Annular
	High (dry out)	Mist

Table 1. Flow patterns in vertical tubes [22].

The Figure 8 shows graphically the different types of flow explained for vertical flows.

Bubbly   Slug   Churn   Wispy-annular   Annular
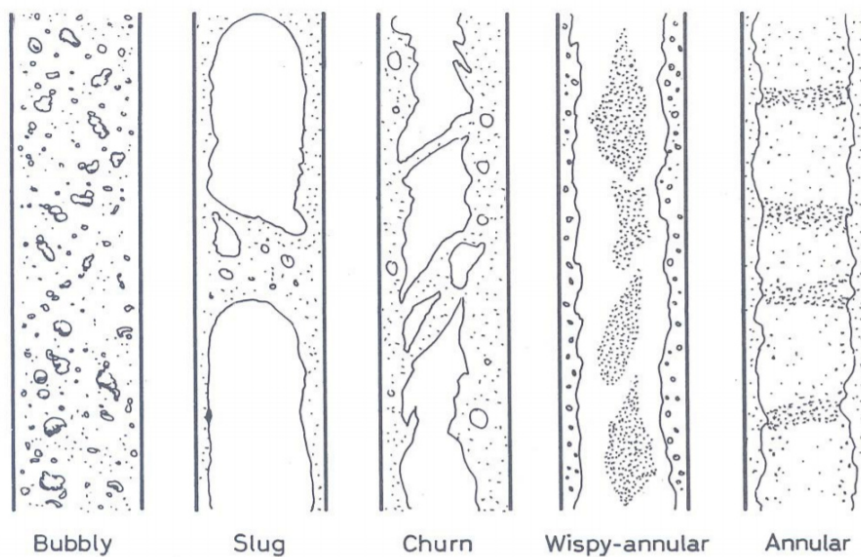
Figure 8. Flow patterns for vertical two-phase flow in vertical pipes. Source: Department of chemical and nuclear energy (Polytechnic University of Valencia) [23]

In case of vertical pipe flow patterns, a differentiation of the flow direction (downflow or upflow) is necessary since the direction of gravity causes a different effect.

The flow patterns that are observed in horizontal or inclined pipes are complicated by the asymmetry of the phases due to the influence of gravity. Some flow patterns are modifications

of those that already existing in vertical flow, but there are others that exist only in the horizontal flow. Flow patterns in horizontal flows tend to be stratified.

1.4.3 Flow patterns for horizontal flow

a) **Bubbly.** It is similar to vertical flow, but with the difference that vapor bubbles tend to flow through the upper half of the pipe.

b) **Plug.** Similar to the slug regime of vertical channels, but with the difference that gas bubbles tend to go through the upper half of the pipe. This flow occurs at moderate levels of void fraction and at slow flow velocities.

c) **Stratified flow.** The two phases flow in a separated form, just attached in a soft way. It only happens at very slow phase velocities for the two phases.

d) **Wavy.** If the gas velocity is increased, the bound layer between both phases is distorted.

e) **Slug.** If the velocity increases further, the interface waves are collected forming a bullet of liquid that moves at high speed.

f) **Annular.** At an even higher gas phase velocities, a gas core with a film of liquid will be formed around the periphery of the pipe. The film can be continuous or non-continuous around the surface, but it will be thicker at the bottom of the pipe, asymmetrically. A part of the liquid phase moves in the form of pulverized flow, being dragged into the gas core in the form of droplets.
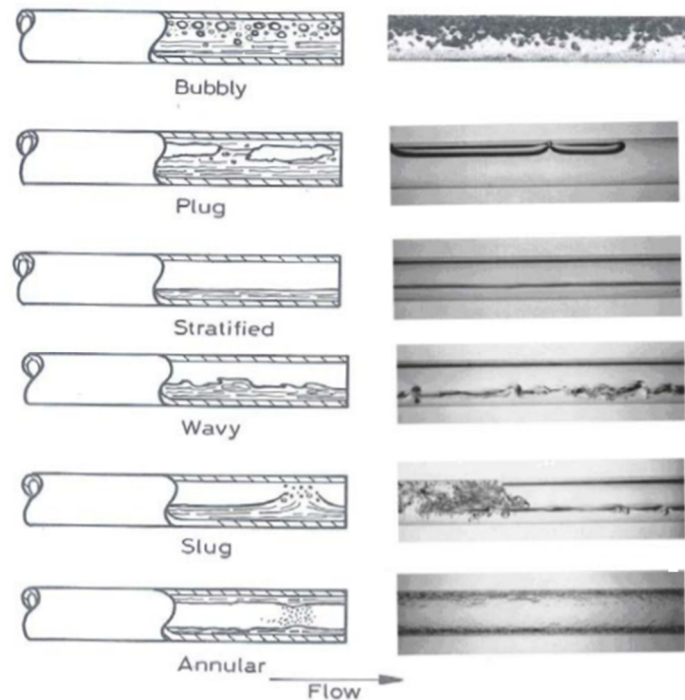
Figure 9. Flow patterns for vertical two-phase flow in horizontal pipes. Source: Source: Department of chemical and nuclear energy (Polytechnic University of Valencia)

The flow pattern determination is so complex and nowadays there is still no general method that has been accepted by everyone. In certain situations, there is no objective way to differentiate between two different flow patterns. Some methods for determining the flow are the flow regime map of Hewitt and Roberts (there are more flow pattern determination maps), or flow regime transition criteria of Mishima and Ishii, both for vertical pipe flow. Another one would be the RELAP code, where the void fraction used for flow pattern transitions is determined using other empirical or semi-empirical models.

1.5 Experimental observation (pattern flow determination)

Although there are methods for the flow pattern prediction, the reality is that the only way to determine the flow pattern is through experimentation. When developing a correlation (with the intention of publishing it), a comparison with the experimental data is necessary. The only thing that can be done, apart from the experimental observation, is to make some assumptions that are not 100% reliable, such as assuming that for a subcooling condition (negative quality) the annular flow pattern cannot happen.

When measuring the flow pattern experimentally, it is important to select properly the instrumentation, since the measuring devices can interfere with the two-phase flow and therefore modify the parameters and the development of the flow along the pipe. There are non-intrusive methods that do not modify the flow characteristics.

Visual observation of the flow is one of the simplest methods that can be used. Through the registration of images of a pipe (Figure 10 shows how flow patterns look in real photos), the existing

flow pattern can be studied. Nevertheless, this method has some drawbacks too. For example, when the area of the pipe is too large, the observation of the flow cannot be done in the center of the pipe. In addition, when the flow is turbulent and the bubbles shake abruptly, it is too difficult to observe the behavior of the flow, unlike when the bubbles move slowly, when the flow can be properly registered. Although usually the experimental determination of the flow is done with visual observation, since there is no other way to do it, the main problem is that in case of high pressures it is practically impossible to carry it out, so the results are not 100% reliable.

There are also other techniques, which are more advanced, in order to measure the flow pattern. These techniques are based on different physical principles to measure flow parameters and flow patterns. Some of these methods are, for example, using the different attenuation of the gamma rays according to the phase (liquid or gas) and its measurement to determine the distribution in the pipe. Another one could be laser technology in order to measure the velocity of the gas phase in the pipe direction; or tracers that are introduced into the flow (in the continuous phase) and are illuminated and detected by an external laser. By this last method the velocity of both phases can be determined in parallel [9].
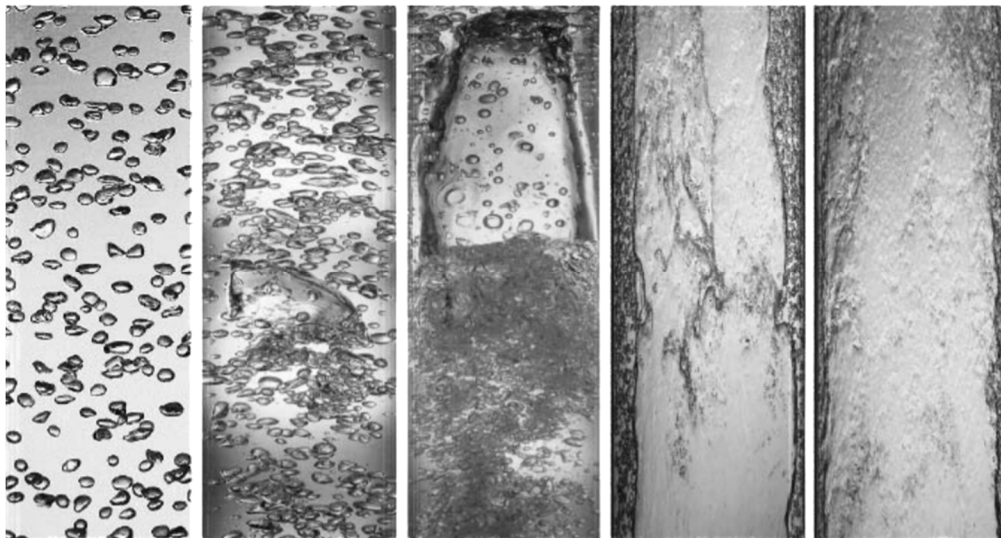
Figure 10. Real picture of flow patterns. Source: Source: Department of chemical and nuclear energy (Polytechnic University of Valencia) [23]

1.6   Review of some flow pattern determination methods

a) **RELAP.** It is a very powerful simulation tool first developed in the national Idaho laboratory and maintained at a later time by the energy department of the Unites States. The RELAP code was developed to simulate and estimate the behavior of the nuclear light water reactor coolant in specific accident conditions. The code used to estimate the flow patterns for vertical flow is displayed in the figure 11. The void fractions used to determine the transitions of the flow are calculated using empirical and/or semi empirical models.
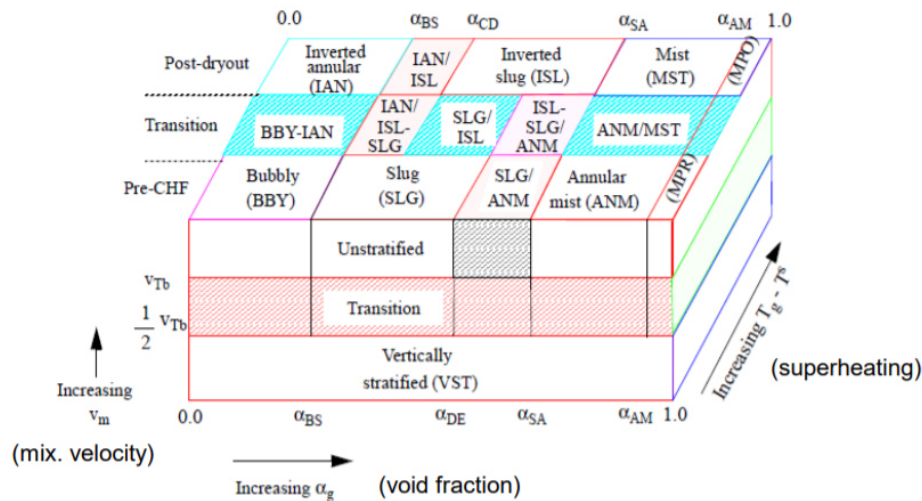
Figure 11. RELAP5/MOD3 of flow patterns. Source: RELAP5/MOD3 Code Manual. (U.S. Nuclear Regulatory Commission)

The Figure 11, correspond to a valid map for every direction flow in pipes with 45º to 90º degrees of inclination. The scheme is tridimensional and show the transitions of the flow pattern considering the void fraction, the average velocity of the mixture and the boiling regime (pre-CHF or post-dryout). The map predict the flow patterns bubbly, slug, annular-mist in pre-CHF and the patterns reverse slug and reverse annular for post-dryout. Despite not being used to predict the flow in the current work, it is important to mention one of the greatest and most used codes in the nuclear engineering.

b) Groeneveld tables. The Groeneveld tables (AECL) allows to make predictions over a wide range of conditions. It is developed from database compiled from multiple published experiments. The database contains more than fifteen thousand points of CHF for the water. The significant advance of this method is how simple and easy to implement it is. Outside from providing the method for CHF prediction, it also provides a database of CHF points to analyze [24].

c) Flow pattern maps. It is often convenient to show the results of studies of flow patterns in terms of maps related to the system parameters. Flow patterns are generally obtained through experimental observation, although there are also maps developed from theory. Many of them, such as the Hewitt and Roberts map are based on the superficial velocities of the two phases; others are based on theoretical works and others on correlations, which allow identification of the boundaries between flow patterns. It is also true that in case of maps that take similar experimental conditions, some contradictions can be found. Probably, it occurs due to the difficulty of distinguishing flow patterns or due to lack of data. Regards to theoretical maps, they are usually not restricted to any type of conditions but, in exchange, they assume some behaviors and processes as ideals.

Some of the most well-known maps are [6]:

- **Unified model for prediction flow pattern transitions for the whole range of pipe inclinations (D.Barnea).** It is a theoretical map that predicts the transitions in steady gas-liquid flow for any inclination of the pipe; therefore, it can be used for vertical flow (upward and downward) as well as horizontal flow. The prediction of the flow pattern is made from the flow rate, the geometry of the pipe (including the degree of inclination) and the properties of the fluid. The Barnea model includes the mechanisms that explain the physical basis for the transitions between patterns [6].

- **Oshinowo and Charles map for vertical down-flow.** It has been obtained experimentally. It is based on the volumetric flow rate of the gas phase and some dynamic properties of the fluid [6].

- **Baker's map.** It is the typical map for horizontal flows. The axes are defined depending on the superficial mass flux or mass velocities of the liquid and vapor [23].
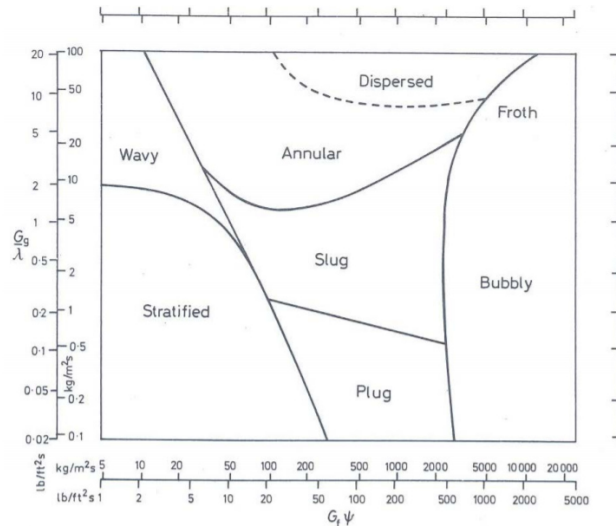
Figure 12. Flow pattern map for horizontal flow (Baker). Source: "Analysis of two-phase flow pattern maps". Brno University of Technology

- **Taitel and Dukler's map for the horizontal flow.** There is also another map of Taitel and Dukler's for vertical flow but it is further (1980). A semi-theoretical map is widely used for horizontal flow. The x-axis represents the Lockhart-Martinelli parameter (dimensionless variable that expresses the liquid fraction) and the y-axis represents the K variable on the left and the T or F variable on the right. Depending on the limit, a different variable is used for the vertical axis (F, T or K). In the following image the axes can be seen properly [6]:
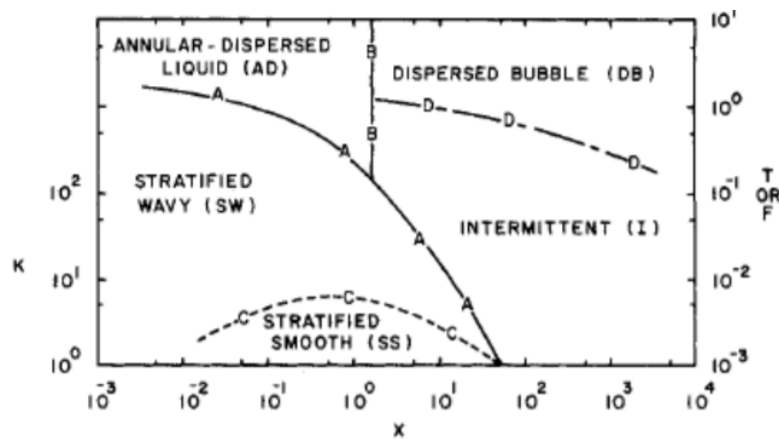
Figure 13. Taitel and Dukler's map for horizontal tubes. Source: "Analysis of two-phase flow pattern maps". Brno University of Technology

- **Hewitt and Robert's map for vertical upward flow.** Taking into account the characteristics of our flow (vertical, upward, small diameter...), the map of Hewitt Roberts has been chosen for the prediction of the flow in the different conditions of the database. The Hewitt and Roberts map is used to identify the flow patterns of a two-phase liquid-vapor flow under particular pressure conditions and for small diameter pipes; therefore, the map is valid for a certain range of data. On the map, each axis represents the superficial

momentum of each phase, that is, the axis represents the square of the phase velocity between the densities for each phase. Map regimes are the flow patterns, which are easily distinguishable, and although clear lines separate them, the transition from one flow pattern to another never occurs suddenly, and each line should really correspond to an area. Concretely, this map has been developed experimentally, and is therefore restricted to the conditions in which it was obtained [6]:
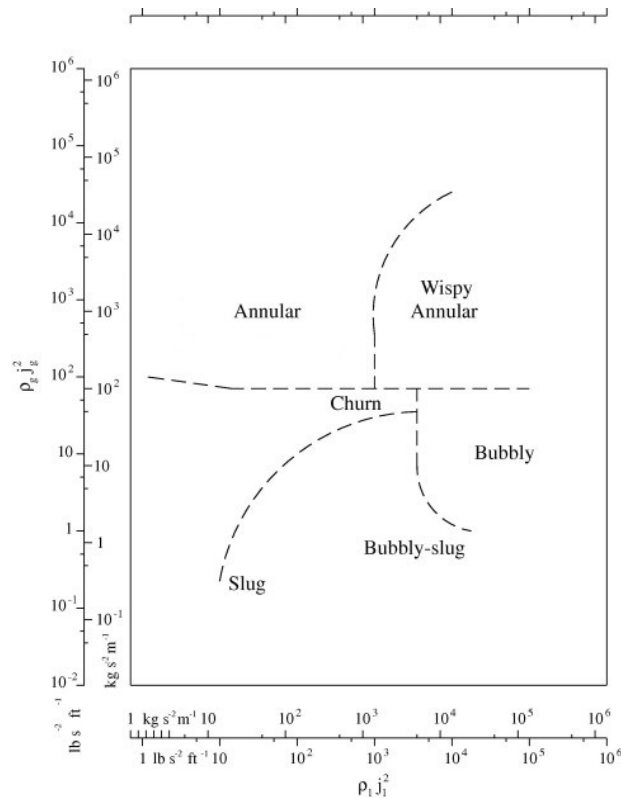
Figure 14. Hewitt and Roberts map for vertical flow. Source: Department of chemical and nuclear energy (Polytechnic University of Valencia)

1.7   Flow pattern transition criteria (Mishima and Ishii)

Flow-regime maps have been a useful tool in order to obtain flow patterns. These flow determination maps are mainly based on the superficial velocities of the liquid and gas, the quality of the flow and the mass flux. The methods that allow to determinate the flow pattern are suitable for slow transitions and quasi-stationary conditions. The reason is that under these conditions, a direct relation between geometric parameters (void fraction) and surficial velocities is assumed. Flow structures depend directly on these geometric parameters, such as the void fraction. In addition, the flow patterns are just classifications of the geometric structures of the flow.

However, the flow pattern determination criteria based on the superficial velocities of the phases cannot be consistent in turbulent flows. This is because the void fraction parameter cannot be determined just from the superficial phase velocities. For a complete two-fluid model, direct geometric

parameters such as the void fraction should be used, instead of the parameters previously used (superficial velocities).

In this criteria of designation of flow patterns, four different regimes have been taken into account: Bubbly, flow, slug flow, churn flow and annular flow.

Bubbly to Slug transition. The transition from Bubbly to Slug is produced due to the agglomerations of bubbles, which join forming a larger main bullet shape bubble. The probability of this phenomenon to occur is very high when the value of the void fraction is around 0.3. This value can be obtained from the consideration of an influence sphere around each bubble (Figure 15), and assuming that the bubbles are distributed in tetrahedral structures. The number of fusions of the bubbles is considered very large when the largest gap between two bubbles becomes smaller than the diameter of the bubble [1].
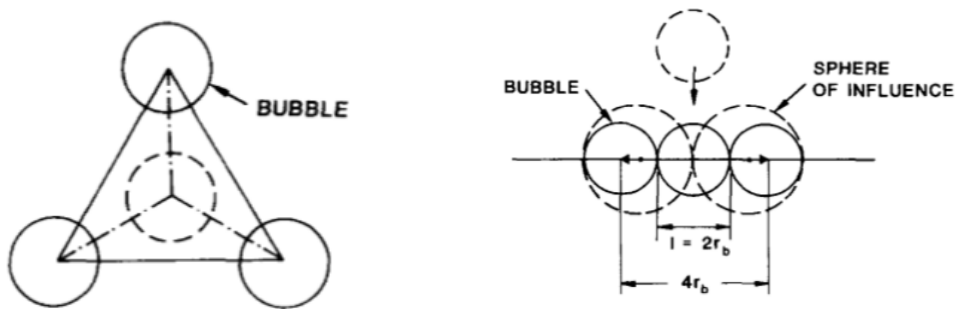
Figure 15. Bubble packing and coalescence pattern. Source: "Flow regime transition criteria for upward two-phase flow in vertical tubes." Kaichiro Mishima and Mamoru Ishii

This condition requires that:

$$\alpha = (2/3)^3 \approx 0.3 \qquad\qquad (11)$$

In order to obtain an equation based on the superficial velocities of the phases, the following equation derived from drift-flux is used [1] [20]:

$$\frac{j_g}{\alpha} = C_0 j + \sqrt{2} \left(\frac{\sigma g \Delta \rho}{\rho_f^2} \right)^{\frac{1}{4}} (1 - \alpha)^{1.75} \qquad\qquad (12)$$

Where:

$$\begin{cases} C_0 = 1.35 - 0.35\sqrt{\dfrac{\rho_g}{\rho_f}} \; for \; recangular \; pipes \\[4mm] \quad C_0 = 1.2 - 0.2\sqrt{\dfrac{\rho_g}{\rho_f}} \; for \; round \; pipes \end{cases} \tag{13}$$

The relation between the superficial velocities of the phases for the Bubbly-Slug transition, taking into account that j is the sum of them, is:

$$j_f = \left(\frac{3.33}{C_0} - 1\right) j_g - \frac{0.76}{C_0}\left(\frac{\sigma g \Delta \rho}{\rho_f}\right)^{0.25} \tag{14}$$

The transition is carried out when the void fraction exceeds the region where the flow is bullet-bubble. Just before the transition occurs, the consecutive bubbles begin to touch each other (bubble tail with the next bubble nose). In this condition the slug flow becomes unstable and the bubbles begin to lose their bubble condition, where the destruction and appearance of bubbles continues (this stage is rather related to a transition stage). The average value of the void fraction along the bubble is obtained by flow analysis until the moment when the flow reaches the void fraction where the flow rate is fully developed. The application of Bernoulli's equation results in the following equation, where h is equal to the distance to the nose [1]:

$$\alpha(h) = \frac{\sqrt{2gh\Delta\rho/\rho_f}}{\sqrt{\dfrac{2hg\Delta\rho}{\rho_f} + (C_0 - 1)j + 0.35\sqrt{\Delta\rho g D/\rho_f}}} \tag{15}$$

The equation associated with the bullet-bubble velocity:

$$v_{gs} = C_0 j + 0.35\sqrt{\frac{\Delta\rho g D}{\rho_f}} \tag{16}$$

Moreover, from different considerations and approximations, the final equation that defines the slug-churn transition is [1]:

$$\alpha \geq 1 + 0.813 \left\{ \frac{(C_0 - 1)j + 0.35\sqrt{\Delta\rho gD/\rho_f}}{j + 0.75\sqrt{\Delta\rho gD/\rho_f}\left(\frac{\Delta\rho gD^3}{\rho_f v_f^2}\right)^{\frac{1}{18}}} \right\}^{0.75} \tag{17}$$

For high flows of the gas phase, the flow pattern becomes annular. The proposed criteria to identify this transition have been developed from two different mechanisms. Flow reversal in the liquid film section along large bubbles, and the destruction of liquid slugs due to deformation or dragging. The first condition, extracted from the first mechanism, can be approximated through:

$$j_g = \sqrt{\frac{\Delta\rho gD}{\rho_g}}(\alpha - 0.11) \tag{18}$$

Where α must satisfy the condition given in the equation that defines the slug-churn transition (equation 17).

The second criteria, obtained from the criteria of the beginning of droplet entrainment is based on the equation [1]:

$$j_g \geq \left(\frac{\sigma g\Delta\rho}{\rho_g^2}\right)^{0.25} N_{\mu f}^{-0.2} \tag{19}$$

Based on:

$$N_{\mu f}^{0.8} = \frac{\mu_f j_g}{\sigma}\sqrt{\frac{\rho_g}{\rho_g}} \tag{20}$$

Where:

$$N_{\mu f} \equiv \frac{\mu_f}{\left[\rho_f \sigma \sqrt{\frac{\sigma}{g \Delta \rho}}\right]^{0.5}} \tag{21}$$

From the transition criteria for the different flow patterns, a map can be drawn for certain conditions and for a given fluid. For example, the Figure 16 shows a map for a water-air flow for certain conditions (Diameter = 25.4 mm, temperature = 25ºC and atmospheric pressure):
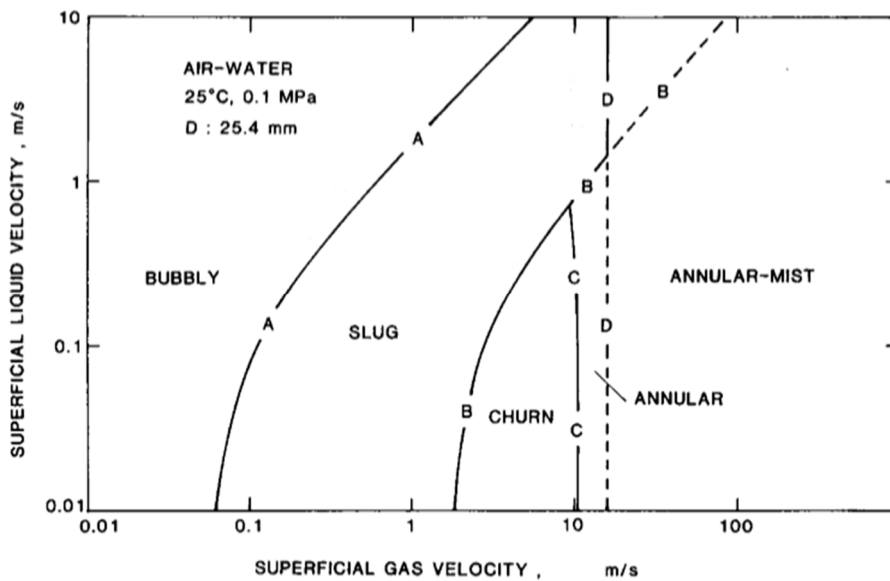
Figure 16. Flow-regime map based on newly developed transition criteria. Source: "Flow regime transition criteria for upward two-phase flow in vertical tubes." Kaichiro Mishima and Mamoru Ishii

The equations developed before represent the boundaries between the regimes. For example, curve A corresponds to the equation of the Bubbly to Slug transition (and its condition). The location of the curves depends on the properties of the liquid phase and the gas phase.

1.8 The Westinghouse correlation for the CHF (W-3).

As mentioned above, the calculation of heat transfer is affected by flow patterns, and at the same time, these flow patterns depend on the effects of pressure, mass flux and flow quality. The pressure defines the saturation temperature (associated with all thermal characteristics) and adapted to the enthalpy provides condensation cooling of bubbles and the latent heat for their formation. The saturation properties, such as viscosity and superficial tension, affect the characteristics of the bubble (size, buoyancy, distribution). The mass flux is related to parameters such as the slip ratio and coolant

mixing. In addition, they affect the size of the bubble layer in the region of low enthalpy (in bubbly flow) or the dragging of liquid bubbles in the region of high enthalpy (in annular flow).

By adjusting the databases available at that moment, in the W-3 Correlation, the mentioned parameters (pressure, quality, mass flux, diameter, and enthalpy) are related by several functions in order to obtain the critical heat flux. Each correlating function was built by plotting the experimental Critical Heat Flux versus an independent parameter with all the other parameters being constant. The W-3 Correlation is a DNB correlation, therefore the results may fit for this type of boiling crisis. The heat flux is an equation as follows [2]:

$$q''_{crit} = F(X,p) * F(X,G) * F(D_e) * F(H_{in}) \qquad (22)$$

Where the functions represent the following:

$$F(X,p) = [(2.022 - 0.0004302p) + (0.1722 - 0.00000948p) \\ * \exp(18.177 - 0.004129p)\,X](1.157 - 0.869X) \qquad (23)$$

$$F(X,G) = (0.1484 - 1.596X + 0.1729X|X|)\left(\frac{G}{10^6}\right) + 1.037 \qquad (24)$$

$$F(D_e) = [0.2664 + 0.8357e^{-3.151D_e}] \qquad (25)$$

$$F(H_{in}) = [0.8258 + 0.000794(H_{sat} - H_{in})] \qquad (26)$$

F (X, p) = Correlating function of coupled quality and pressure effects on CHF.

F (X, G) = Correlating function of coupled mass flux and quality effects on CHF.

F (D_e) = Correlating function of hydraulic diameter effect on CHF.

F (H_{in}) = Correlating function of inlet enthalpy effect on CHF.

The equation is written in British units; therefore, the pressure is expressed in *psia*, the mass flux in *lb / hr ft²*, the diameter in *inches* and the enthalpy in *Btu / lb*. The quality is dimensionless.

Note that this correlation can only be used correctly for specific ranges:

Parameter	Range
Pressure	[1000 - 2300] psia
Mass flux	[1·10⁶ - 5·10⁶] lb/hr ft²
Diameter	[0.2 – 0.7] inches
Quality	X ≤ 0.15,
Inlet enthalpy	Hin ≥ 400 Btu/lb
Length	[10 – 144] inches
h/w per	[0.88 – 1]

Table 2. Range for the application of W-3 correlation

Where h/w per = heated perimeter/wetted perimeter

The W-3 correlation is used to calculate the CHF for a uniform heat flux. To calculate the CHF for non-uniform heat flux, it is necessary to apply the called F-factor.

$$q''_{crit\,non\,uniform} = \left(\frac{q'_{crit\,EU}}{F_C}\right) \tag{27}$$

Where:

$$F_c = \frac{C}{q_{loc}[1 - \exp(C * l_{DNB,EU}]]}\int_0^{l_{DNB,non}} q''(z)\exp[-C(l_{DNB,non} - z)]dz \tag{28}$$

With the coefficient C, equal to:

$$C = 0.15 * \frac{(1 - X_{DNB})^{1.31}}{(G/10^6)^{0.478}} \ (l/in) \tag{29}$$

X_{DNB} = Quality at DNB location under uniform heat flux conditions.

$l_{DNB,\,EU}$ = axial location at which DNB occurs for uniform heat flux.

$l_{DNB,\,non}$ = axial location at which DNB occurs for no uniform heat flux.

The Figure 17 shows the accuracy of the W-3 Correlation. The dispersion values are represented.
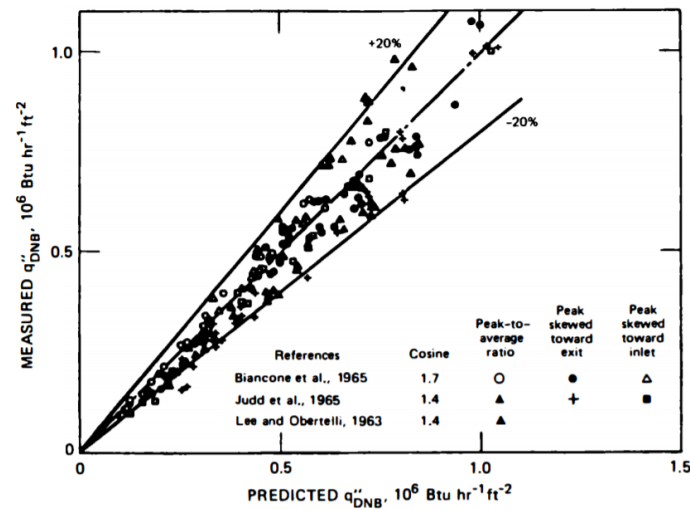
Figure 17. Comparison of W-3 prediction and data with non-uniform fluxes. Source: "Boiling heat transfer and two-phase flow". L.S. Tong and T.S. Tang

1.9   Implementation tool

The tool used to program all calculations, prediction methods, graphics, function creation, statistical analysis, and, in short, everything necessary to carry out the project has been Python. Python is an interpreted programming language whose advantages are its accessibility, flexibility and its large number of libraries available. Then, there is a brief explanation of the libraries that have been used to carry out the programming:

a) **Pandas.** It is an open resource for database manipulation and analysis. It is written as an extension of NumPy, which is a library with high-level mathematical functions. Using this library, the database used for the creation of new variables, manipulation of the existing ones (such as unit changes), creation of categorical variables, counting of the number of variables of each type, data filtering, creation of new databases... has been manipulated. Practically, all the manipulation of the data carried out in this project has been done with the Pandas library.

b) **Matplotib.** Matplotlib has been the library used to generate graphs, diagrams and everything related to 2D data plotting.

c) **Seaborn.** This library has been used to perform the statistical visualization of the data. It is based in matplotlib, but it is used instead of matplotlib because a couple of features, for example, the plotting of the boxplots.

d) **Sklearn.** To the creation of the regression models and the calculation of the accuracy and quality of the model.

e) Statsmodels. It is a module of Python that will help to implement different statistical models. It has been used to perform specific test like ANOVA.

f) IAPWS Library. In order to calculate the properties of the water phases, the IAPWS library has been used, which implements in Python the standards of the International Association for the Properties of Water and Steam. This organization is interested in the properties of water and vapor (thermophysical properties and other aspects of water/vapor at high temperatures) relevant for the production of thermal power in industrial and research applications. From this organization, the necessary information about the formulation of water properties, which is accepted internationally, is extracted, as well as the actual technical information on energy production and other industrial applications.

This information is relevant when calculating certain parameters, which are necessary for the calculation of heat flow, for example, in the W-3 correlation for density calculation, or in the Mishima transition criteria where density, superficial tension or viscosity are required parameters for the determination of the flow pattern.

2. Analysis

2.1 Analysis of the data used

For the analysis and the realization of the tests, a database composed initially of five parameters has been used. The information found in the database is information regarding the local parameters at the CHF location. The database consists of 7245 lines x 5 parameters. The data is extracted from the Groeneveld look up tables [24].

Pressure	Mass flux	Quality	Heat flux measured	Flag
MPA	Kg/m^2s	Dimensionless quantity	Kw/m^2	Categorical variable
[0.1,21]	[0,8000]	[-0.5,1]	[0,44338]	

Table 3. Units of the data

The flag variable represents the method used to obtain the heat flow measurement. There are four different methods and each of them is represented with a different color:

White	Experimental data (less uncertainty of the data)
Green	Prediction methods neighboring experimental data conditions

Red	CHF values impossible to obtain. They are used to improve interpolation accuracy of other regions.
Blue	Limited Quality region (LQR) where rapid changes in CHF vs Quality curve can be obtained

Table 4. Meaning of the tag variable

Data with red flag variable will not be used as data because they are not real parameters and because of that, the results could be wrongly altered. From the beginning of the use of the data, the lines with flag red variable have been discarded. Note that the database with flag white variable is the most reliable, since it has been obtained directly from experimental conditions.

The Figure 18 shows the flag variable distribution:
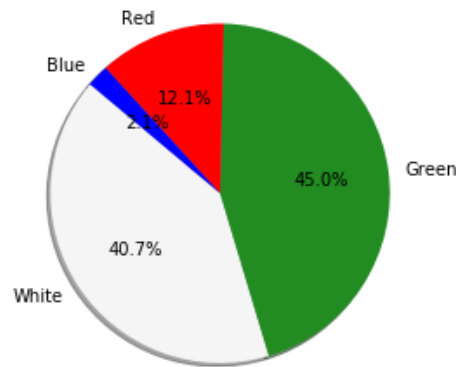
Figure 18. Layout of variable tag

Non-useful variables do not make up more than fifteen percent of our total database (877 lines).

Another important thing from the database that is important to mark is that the values of pressure, mass flux and quality, despite being continuous variables that can take any value, take fixed values. In other words, between the range of numbers that each variable can take, they take certain values that are repeated for a given number of lines in which the other two variables change.

Aside from the parameters of the database and the parameters extracted by calculation from the initial parameters, the development requires some other variables, which are necessary [24]:

Inside diameter = 8 mm	e constant = 2.71828182845904	g constant = 9.8

The Pandas library, built in the Python programming language, has been used to manipulate the database. There is no null value within the database.

As explained above, one of the heat flux calculation methods used is based on the use of correlations, like the mentioned Westinghouse correlation for the CHF (W-3). The objective of the incoming analysis is to observe how this correlation works and how provides the result. The comparison with the obtained flow regimes using the proposed prediction methods is a key to analyze the results. In this

way, a more complete analysis of the correct operation of the correlation for different flow patterns and for different groups of variables (by creating categorical variables) can be presented. These new variables can be tested to analyze if they are significant in the flow calculation. Apart from this, interesting conclusions may be drawn beyond predicting heat flow.

From the correlation analysis, a multiple regression can be carried out to predict the heat flow of the selected data group. Based on the experimentally measured heat flux, the success of the regression can be determined using the ratio of error and the comparison.

As a first method, the Hewitt and Roberts map has been implemented in order to predict the flow pattern. Then, the Mishima-Ishii method has been used as the second method of flow pattern estimation. Regarding the Hewitt and Roberts map, it is significantly worse than the Mishima method. The main reason is that it is developed with less data; also, it is simpler and older, considering the second method more reliable than the first.

2.2 Implementation of the first prediction method. Hewitt and Roberts map

The Hewitt and Roberts map used for the determination of the flow regime is based on the calculation of two coefficients for each flow state, being this map valid for small diameter pipes.

The value of the coefficients is as follows:

$$Fcoef = \frac{((1-x)G)^2}{\rho_l} \tag{30}$$

$$Vcoef = \frac{(xG)^2}{\rho_g} \tag{31}$$

While the *Fcoef* coefficient is represented on the x-axis, the *Vcoef* coefficient is represented on the y-axis (Figure 19). The coefficients represent the superficial moments of the two phases.
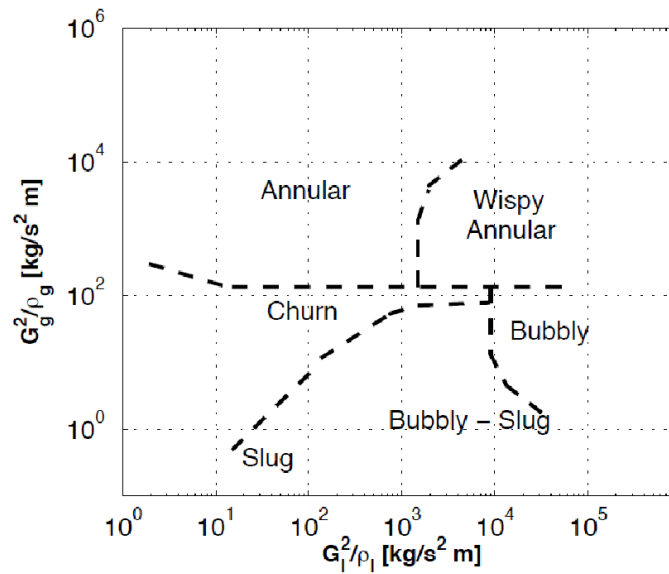
Figure 19. Hewitt and Roberts map. Source: "Two-phase flow patterns maps for macrochannels." Thome, John and Cioncolini, Andrea

As part of the flow determination, it is necessary to calculate the coefficients and mark the point on the map. According to the area in which the point is located, the flow pattern can be obtained. This map can be also found without the line that represents the border between Wispy Annular and Annular.

In addition, each line, which acts as a boundary between flow patterns, has been obtained experimentally, and therefore they do not match to any function. In order to implement this method, several functions in different ranges have been built and from these built functions, the area where the point is located without the need for observation can be determined.

The approximations are good enough for the proper functioning of the map, especially if considering, that in fact, the horizons between flow regimes are diffuse, and they are not, in any case, a perfectly defined line that represents the sudden change from one pattern to another. In addition, the flow pattern is sometimes a subjective judgment.

The functions that have been used to define the boundaries of the map are the following:

a) **Range Vcoef** = [100, 1e5] kg/s2m

   I) Boundary Annular – Wispy Annular

$$Vcoef = 8432{,}5 * Ln(Fcoef) - 59627 \qquad (32)$$

b) **Range Vcoef** = [48, 100] kg/s2m

I) Boundary Churn – Bubbly

$$Fcoef = 5070$$

c) **Range [10, 48]**

I) Boundary Churn – Slug

$$Vcoef = 10.599 * Ln(x) - 36.261 \qquad (33)$$

II) Boundary Slug – Bubbly

$$Fcoef = 5200$$

d) **Range [0, 10]**

I) Boundary Churn – Slug

$$Vcoef = 0.0043 * Fcoef^{1.7405} \qquad (34)$$

II) Boundary Slug – Bubbly

$$Vcoef = 139342 * Fcoef^{-1.164} \qquad (35)$$

These functions are the representation of the boundaries between regimes. To complete the coefficients calculation, the quality and mass flux are acquired from the database. The density of the liquid phase and the density of the gas phase is obtained from the IAPWS95 tables; from the value of the pressure and the value of quality (quality equal to zero for the density of the liquid, and quality equal to one for the density of the gas).

Thus, Hewitt and Roberts maps with the coefficients located are represented in this way:
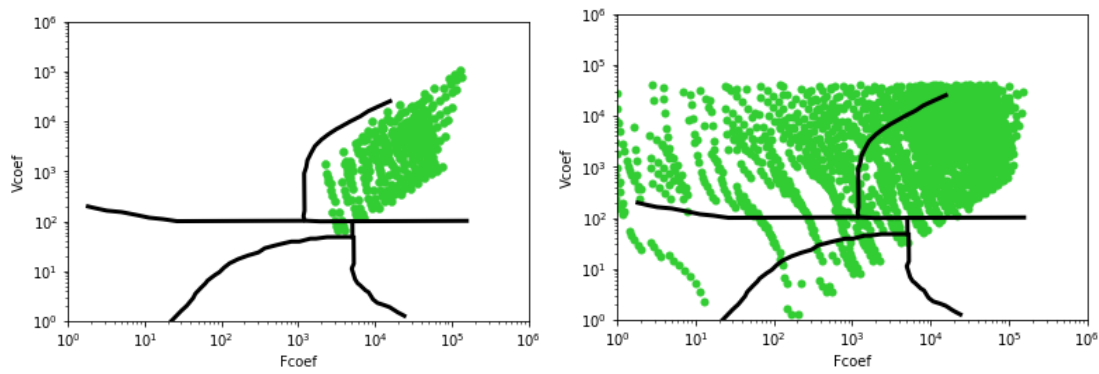
Figure 20. Distribution of the data in the Hewitt and Roberts map for filtered and non-filtered data

On the one hand, the first graphic belongs to the filtered database in which there are only data within the performing range of the correlation and directly experimental obtained.

On the other hand, the second graphic corresponds to the complete database, with the exception of the initially filtered values that corresponded to data, which are impossible for the critical heat flow. A top cut is also observed in the second graph data. It is performed in order to prevent the data from leave the map's operating range. Using the following bar chart, the amount of data with each flow pattern can be observed:
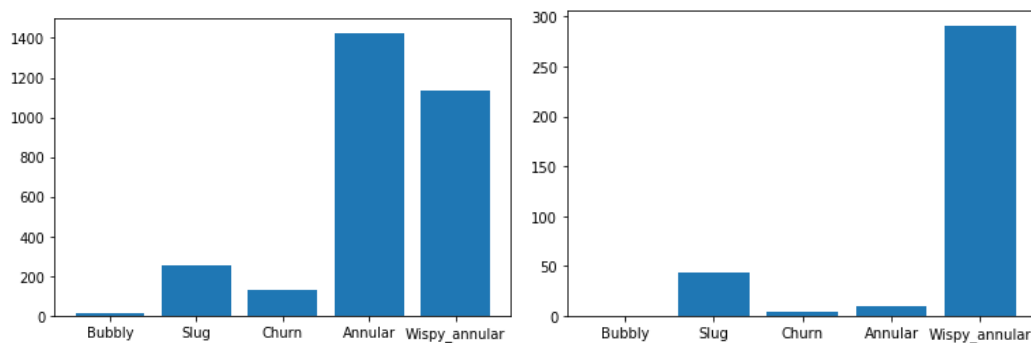
Figure 21. Distribution of the flow pattern predicted by the Hewitt and Roberts map

Once we have the functions that represent the barriers between regimes, plotting the coefficients is unnecessary but according to this prediction method, it allows us to have a view on the predominant/main regime in the database

As mentioned above, according to this method, the prediction depends just on the coefficients of each phase, and therefore, there are no conditions that limit the area where a point can be found (related to the parameters). This observation is important, since there a flow regime that can be predicted for conditions in which the flow regime cannot occur (due to theoretical conditions). This completes the first prediction method of the flow regime of the database.

2.3 Implementation of the second prediction method. Mishima and Ishii method.

The second prediction method used is the flow regime transition criteria upward two-phase flow in vertical tubes developed by Mishima and Ishii. This method consider five different flow regimes (Bubbly, Slug, Churn, Annular-Mist and Annular) and it is a more complex (and later) method than maps.

To carry out the method of Mishima and Ishii and using the variables in the database, it is necessary to calculate the superficial velocity of each phase. The density parameters (liquid and vapor phase), surface tension, kinetic and dynamic viscosity have been obtained directly from the pressure and flow quality through the IAPWS95 library.

From this point, the following procedure has been followed for the superficial velocities calculation [7]:

a) **Void fraction calculation:**

$$\alpha = (\frac{C_0}{\alpha_{hom}} + \frac{\rho_g * u_{gj}}{\dot{x} * G})^{-1} \qquad (36)$$

Where:

$$\alpha_{hom} = \frac{\rho_l * \dot{x}}{\rho_l * \dot{x} + \rho_g * (1 - \dot{x})} \qquad (37)$$

The coefficients are calculated as follows:

$$C_0 = 1 + 0.2 * (1 - \dot{x}) * \frac{(g * d_h)^{0.25} * \rho_l^{0.5}}{G^{0.5}} \qquad (38)$$

$$u_{gj} = 1.18 * \left(g * \sigma * (\rho_l - \rho_g)\right)^{0.25} * \frac{(1 - \dot{x})}{\sqrt{\rho_l}} \qquad (39)$$

42

b) Slip ratio calculation:

$$S = \frac{\dot{x}}{1 - \dot{x}} * \frac{1 - \alpha}{\alpha} * \frac{\rho_l}{\rho_g}$$

(40)

I)   Phase velocities calculation:

$$w_g = \frac{G}{\rho_l} * S * \left(1 + x * \left(S * \frac{\rho_l}{\rho_g} - 1\right)\right)$$

(41)

$$w_l = \frac{G}{\rho_l} * \left(1 + x * \left(S * \frac{\rho_l}{\rho_g} - 1\right)\right)$$

(42)

II)   Final calculation of superficial velocities:

$$w_{gs} = w_g * \alpha$$

(43)

$$w_{ls} = w_l * (1 - \alpha)$$

(44)

It is necessary to specify some things that have been done when implementing these equations in the program. Notes:

I.   When calculating the void fraction, the above formula has only been used for the quality range (0, 1). When the quality is equal to one, the void fraction is equal to one, and when the quality is equal to zero, the void fraction is equal to zero. The relationship can be seen in the Figure 22:
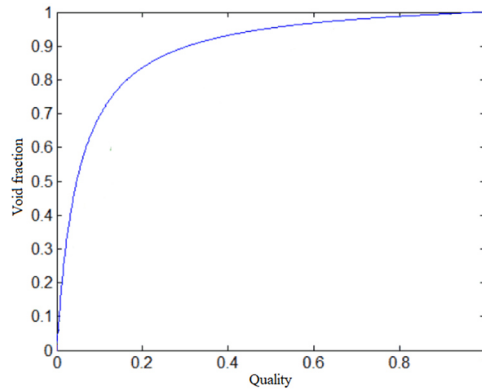
Figure 22. Relation between void fraction and quality (water 7 Mpa)

II.   For a negative quality, the equation of the void fraction is not valid (the negative values of void fraction do not have sense). In order to calculate the void fraction at those values, it is necessary to make an estimation of its value in the subcooled flow-boiling zone. It is a complex estimation that is not worth considering the purpose of the prediction method. The reason is that, for a negative quality, it only can exist bubbly flow according to the equations proposed by Mishima and Ishii. Hence, in order to perform the implementation, for all the negative values of quality, bubbly patter is assumed. And, in that case, it is not necessary to calculate the superficial velocities to determine the flow pattern (the flow pattern is already predicted as bubbly)

III.   When calculating the Slip ratio, the formula does not make sense for quality values equal to one. The slip ratio parameter corresponds to:

$$S \equiv \frac{v_v}{v_l} \qquad (45)$$

Because of that, it has been assumed that when the quality is equal to zero (and the entire flow is liquid) the slip ratio takes the value of one, since the vapor velocity is in the numerator of the fraction. Nevertheless, when the quality is equal to one (all the flow is vapor) the Slip ratio does not make sense, as can be seen in the previous fraction, the zero referring to the liquid velocity is in the denominator. This has been implemented in the program as follows: when X = one, the value of Slip ratio is equal to the character "vap" instead of a number, essentially because there is no two-phase flow in general.

Once the superficial velocities of each phase have been calculated, the flow rate can be predicted according to the Mishima-Ishii method.
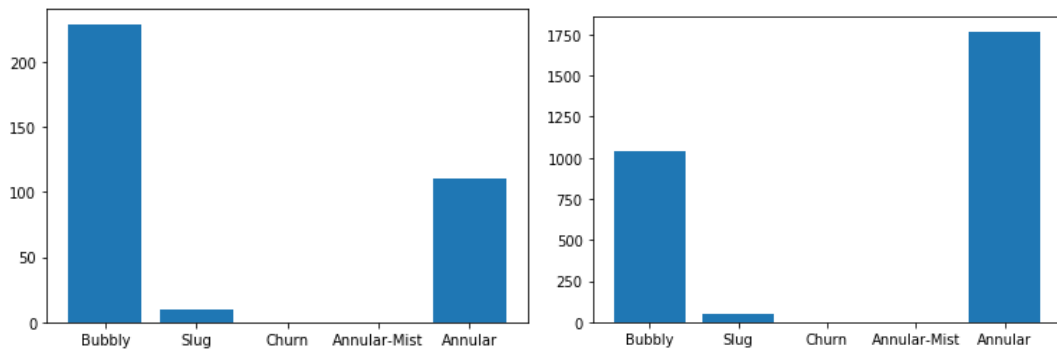
Figure 23. Distribution of the flow patterns predicted by Mihisima method for the filtered and non-filtered ata

The graphs represent the participation of each flow regime. The first graph corresponds to the filtered data obtained in an experimentally direct way in the correlation range. The second graph contains the data obtained experimentally directly.

It is logical that the first chart has a distribution where the Bubbly regime is predominant, unlike the second one. It is due to that the correlation is theoretically for the DNB type CHF, which occurs for low qualities. Filtration has been done in order to use the correlation properly, so the values provided are reliable, therefore, high qualities where the bubbly regime is less likely to occur have been eliminated in the filtrate.

Thus, with the flow pattern determination, a new categorical variable has been inherently created. From this categorical variable, we can study what influence, if there is, has the flow regime flow in the heat flux. According to the exposed theory, the influence is enormous due to the change in the heat transfer mechanisms, but thanks to the statistical analysis, it is possible to see how big this influence is and how much it affects each flow for the present database.

In spite of that, this is not the only categorical variable that can be created. Pressure, quality and mass flux can also be grouped into pools of high, medium or low in order to evaluate how they affect heat transfer. Although it is also true that the creation of these groups is not trivial. The importance remains in the ability to recognize for which ranges it is more likely to appear certain physical phenomena. In the same way as the flow patterns are not randomly determined, the subdivision into groups of a specific variable must be done conscientiously.

The chosen test to observe if there are meaningful differences between the different flow patterns is mainly the ANOVA (Analysis of variance) test. The ANOVA test is a set of procedures and statistical models used to analyze the differences between the means of the groups in a sample of data. In the ANOVA test, important assumptions are made that have to be fulfilled in order for the p-value (result) to be valid [16]:

1. The samples are independent.
2. Each group is from a data with a normal distribution.
3. The variance of the groups are equal.

In order to reach the reliability of the results, the conditions must be accomplished. Moreover, to verify that the groups have equal variances, the Barlett test can be realized. If the sample does not have a normal distribution, the check will be done using the Levene test, which is a more robust test.

Once the check has been done and if the number of groups is equal to two, the T-test can be used. The test is used, like ANOVA, to check if the averages of two groups are equal. When the number of groups is higher than two, then instead of using the T-test, the ANOVA used.

If the conditions assumed are not met, other test tests should be used. On the one hand, in case of having only two groups, the non-parametric test that can be used is the Welch test, which allows to verify the differences in the average of two groups. The Welch test is the homologous test to the T-test but when there are more than two groups. On the other hand, if there are more than two groups (and the ANOVA conditions are not met), the Kruskal-Wallis test can be used. The Kruskal-Wallis test is a non-parametric version of the ANOVA test. The samples in Kruskal-Wallis can have different sizes [25].

These tests are important because using a test when conditions are not met can distort the results and invalidate the hypotheses obtained from them.

If the ANOVA test result shows significant differences between the groups, it is important to determine between which groups these differences exist. To do it, the Tukey test is used, which is a test to find between which groups the difference is significant. There is an alternative method, which can also be used for this proposal, the Holm-Bonferroni

For these tests, the *p-value* shows if the null hypothesis of each test can be rejected, and, therefore, finds if there are significant differences between the groups. In the case that the *p-value* is lower than the 0.05, there are differences; we assume that we can reject the null hypothesis. The value has been set at 5% (commonly used value).

The analyzed groups contain the data of the experimentally measured heat flux for each categorical variable.

2.4 Categorical variable analysis. Flow pattern

In order to analyze the different flow patterns predicted by the methods and validate the theory, it is necessary to perform the aforementioned statistical tests.

First, the data chosen is the one adjusted to the W-3 Correlation. In order to have an idea of the distribution of the data, a suitable graphic is the boxplot:
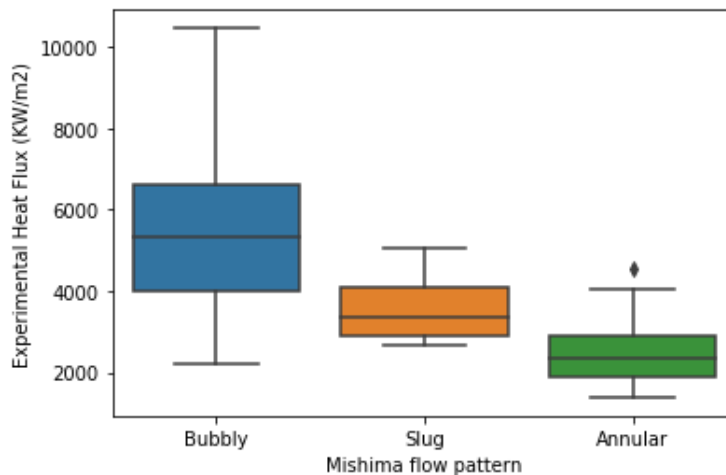
Figure 24. Boxplot of the heat flux for the flow patterns predicted

As seen in the Figure 24, there are significant differences between flow patterns. At first sight, it can be seen that the greatest heat transfer is in the Bubbly flow and the lowest in the annular flow. This result is consistent with the theory, which predicts a reduction in the heat transfer coefficient for an annular regime where boiling film is produced, compared to the Bubbly regime.

In any case, it is not possible to validate the hypothesis just through the observation of the graph. It is necessary to perform the tests to be able to affirm that there are differences and complement the graph.

The test result is the folllowing:

Statistic = 193.30307	p-value = 1.058692395e-42

Considering the p-value, the null hypothesis of the test is rejected. The average of the database for the two groups is different, so it can be affirmed that there are differences between the groups. The mentioned fact is something expected that is confirmed by the test. On this basis, it is necessary to know between which groups the differences are found. First, it is decided to make changes in the treatment of the data groups in order not to obtain false results.

The group that includes the Bubbly flow pattern is too large. When determining the Bubbly flow, as shown above, two conditions have been imposed. The first condition is that which is determined by the Mishima method and corresponds to a void fraction less than 0.3. The second one, it is based on an assumption in which when the flow acquires a negative value (subcooled boiling) the flow pattern that occurs is the Bubbly pattern, so, all data with negative qualities have been identified with the Bubbly regime. Consequently, after observing the amount of data with each regime, a new pool of the data has been devised. The Bubbly flow with negative quality has been separated from the bubbly flow associated with a positive quality, which has been obtained from the relative condition of the void fraction. Instead of working with a single group associated with the Bubbly flow pattern, it is decided to work with two.

The new box diagram that represents this grouping is as follows:
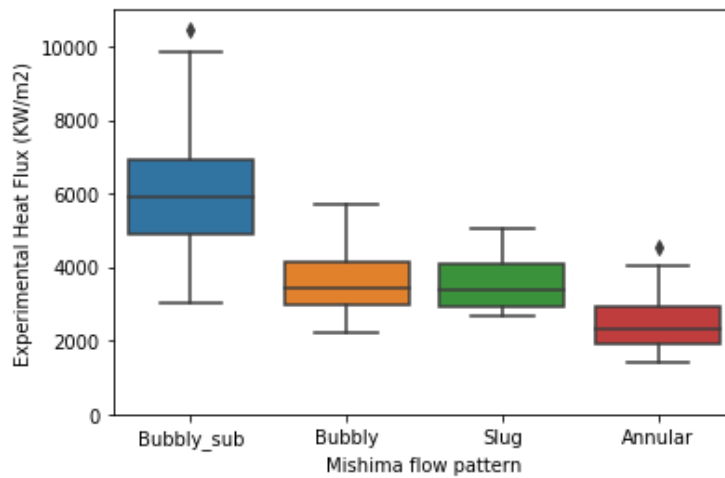
Figure 25. . Boxplot of the heat flux for the flow patterns predicted, with the addition of the new bubbly group

Now the size of the Bubbly box has been divided into two. In the new distribution differences between the groups can be appreciated, but the average of the groups is much closer. As in the previous case, a test is carried out to evaluate differences. For these groups, there are differences in the standard deviation and therefore, the test carried out to observe if there are differences between the groups is the Kruskal-Wallis test:

Statistic = 249.66440	p-value = 7.73411984e-54

The p-value is extremely small, almost zero, which indicates that the statistical difference between the groups is obvious. After this, it is necessary to make the Tukey test to the groups to observe between which groups the difference is found. Tukey test:

```
================================================================
  group1      group2    meandiff  p-adj    lower      upper    reject
----------------------------------------------------------------
   Annular      Bubbly  1138.7753  0.001   621.9237  1655.627    True
   Annular  Bubbly_sub  3564.9933  0.001  3181.0421 3948.9445    True
   Annular        Slug  1139.2182 0.0254    99.3064 2179.1299    True
    Bubbly  Bubbly_sub   2426.218  0.001  1942.1539 2910.2821    True
    Bubbly        Slug     0.4429    0.9 -1080.4438 1081.3295   False
Bubbly_sub        Slug -2425.7751  0.001 -3449.7863 -1401.764    True
----------------------------------------------------------------
```

Table 5. Result of the Tukey test for the flow pattern groups

A result equivalent to the true value in the reject column means that there is a significant difference between the groups. In the table, it can be seen that there are significant differences between all the groups, except for the groups bubbly and slug. These differences are the most logical result, although having in mind some differences (it is also important consider that, from some points of the database

the flow pattern may be diffuse). It is marked that the difference between the heat fluxes varies depending on which are the groups analyzed. Thus, the differences between the pattern bubbly and the pattern slug are so much lower (there actually no almost no differences) rather than the differences between annular and bubbly. This may be due to the physical distribution and shape difference between one pair of groups is totally different regarding the other pair of groups. It is not surprising that the non-existing difference is pointed for the relation between the groups bubbly and slug. Furthermore, if considering that pattern bubbly and slug are sometimes indistinguishable, especially in the non-subcooled region. And here it is observable that in the case in which there is only a bubbly pattern, the difference do exist:

```
group1 group2  meandiff  p-adj     lower       upper     reject
---------------------------------------------------------------
Bubbly   Slug  -1832.4642  0.001  -2961.1221  -703.8063    True
```

Table 6. Difference between Bubbly and Slug

Another thing to consider is that the sample of the slug flow in the data selected is perhaps too small since the filtering was disposed to perform the best results for the W-3 correlation.

Therefore, in order not to leave the analysis of the relationship between the flow regimes and the heat flow unconsidered, it is important to perform again this same test, but for the entire database (just filtering the impossible values). Box diagram for the entire database (almost ten times larger):
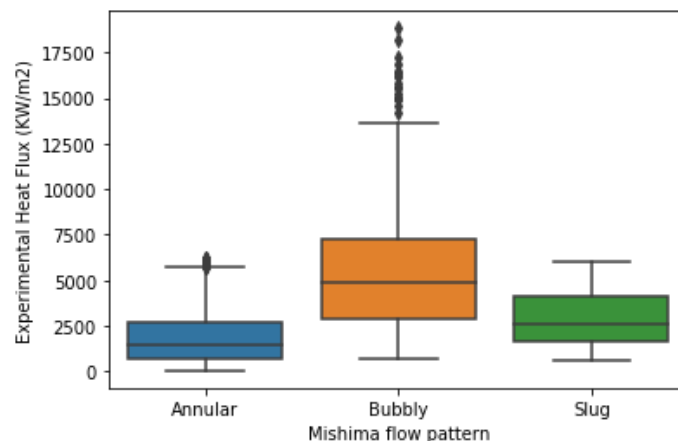
Figure 26.Boxplot of the heat flux for the flow patterns predicted (non-filtered data)

In this boxplot, more data that are atypical that do not meet a certain homogeneity are observed. It is not worrying since the data is bigger and there is no specially filtering at all. There are as well differences between the pattern groups. The higher heat flux is more likely to be grouped in the bubbly group (as it should be according to theory), while annular group contains the data with the lower heat flux. The statistical test that confirm that:

Statistic = 840.86966	p-value = 7.870302538e-288

The p-value is almost zero, so it is necessary to find the groups in which the difference is relevant; and for that, the Tukey test is used:

```
        Multiple Comparison of Means - Tukey HSD, FWER=0.05
=====================================================================
 group1 group2  meandiff  p-adj     lower       upper    reject
---------------------------------------------------------------------
Annular Bubbly  3569.5306  0.001   3365.3682  3773.6931   True
Annular   Slug  1030.2585 0.0029    295.8581  1764.6589   True
 Bubbly   Slug -2539.2722  0.001  -3281.0313 -1797.513    True
---------------------------------------------------------------------
```

Table 7. Results of the Tukey test for the flow pattern groups (data filtered for the correlation)

According to the Tukey's test, there is a relevant difference between all the groups formed. That is more reasonable theoretically speaking. The larger the size of the data, the better the results are obtained, and this can be seen in the previous analysis compared to this one.

In order to continue with the previous data processing, now the bubbly group is divided in two subgroups like before. The new resulting boxplot is:
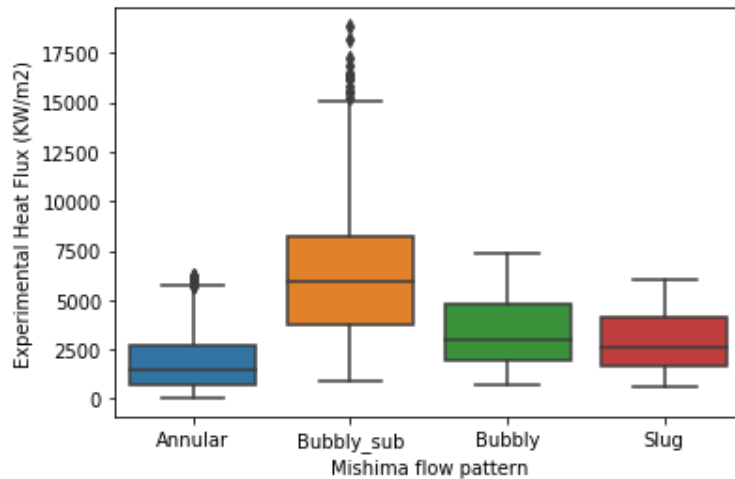
Figure 27. Boxplot of the heat flux for the flow patterns, with the new bubbly group (non-filtered data)

With the relevant test to see the differences:

Statistic = 1159.2435632462	p-value = 5.1034070676e-251

The p-value is almost zero, hence, the difference between the new groups for the full data exist. As it has been previously done, it is mandatory to check between which groups the difference is significant:

```
===================================================================
  group1      group2    meandiff   p-adj     lower       upper    reject
-------------------------------------------------------------------
   Annular      Bubbly  1641.8867   0.001  1320.7659   1963.0076    True
   Annular  Bubbly_sub  4465.2861   0.001  4227.4236   4703.1486    True
   Annular        Slug  1030.2585  0.0025   277.7676   1782.7494    True
    Bubbly  Bubbly_sub  2823.3994   0.001  2466.5514   3180.2473    True
    Bubbly        Slug  -611.6282  0.1997 -1409.7538    186.4974   False
Bubbly_sub        Slug -3435.0276   0.001 -4203.4444  -2666.6108    True
-------------------------------------------------------------------
```

Table 8. Results of the Tukey test for the flow pattern groups with the new bubbly group (filtered data)

Among all the groups there are significant differences except once again for the couple formed by Bubbly and Slug. Considering all the strong relations that may exist between the groups, this one is probably the most understandable. Sometimes it is not even possible to differentiate the bubbly flow from the slug experimentally; the boundary is usually generally diffuse. It is usual that the heat transfer does not suffer relevant changes between the two groups.

It might be said that the last tests and their conclusions are more valid than the tests performed at the beginning since they have a bigger base data, and the atypical points affect less the analysis. Even so, the filtered data analysis for the W-3 correlation is necessary for the subsequent sections of the work, where the correlation will be analyzed to figure out which flow regimes are more valid and where the correlation fails more frequently (considering that, the W-3 correlation is for the DNB type).

It can be argued that the results are largely satisfactory. The differences in heat flux for different flow patterns have been showed in the plots and confirmed by the tests. Despite not being a huge database, the data has been useful to validate some of the points indicated in the introduction as a fundamental part of the critical heat flux review. Moreover, it is evident that, if everything goes correctly, for the implemented program, when using a larger database (setting the limits thoroughly) the results will be the same; and they will serve to ratify even more clearly the changes in heat transfer according to the distribution of the phase.

2.4.1 Quality categorical variable analysis.

This section aims to assess the influence of the quality of the flow on heat transfer. The value of quality defines the type of boiling crisis. For lower qualities, the DNB phenomenon appears, while for higher qualities the phenomenon known as dryout appears. Even so, it is not known whether there is an exact range for which one phenomenon or another occurs. Therefore, it could be said that the lower the quality, the higher the probability that the DNB phenomenon will appear, while the higher the value of the quality, the higher the probability that the dryout will appear. In the region of medium quality, the two phenomena are possible. In addition, it is generally assumed that dryout occurs when the regime is annular [2].

Then, according to the previous considerations, the decision that has been taken to categorize the quality variable is to associate the Bubbly flow with the categorical variable of quality "low", and, on the other hand, associate the Annular flow with the categorical variable of "high" quality. The

remaining values that do not correspond to either Bubbly or Annular have been subdivided according to their quality for a limit value of 0.05. This value equivalent to 5% approximates the limit between the two high and low zones (although this limit does not really exist).

Before proceeding to this subdivision, it is important to visualize the quality data to see if the distribution that follows this data is close to a normal distribution:
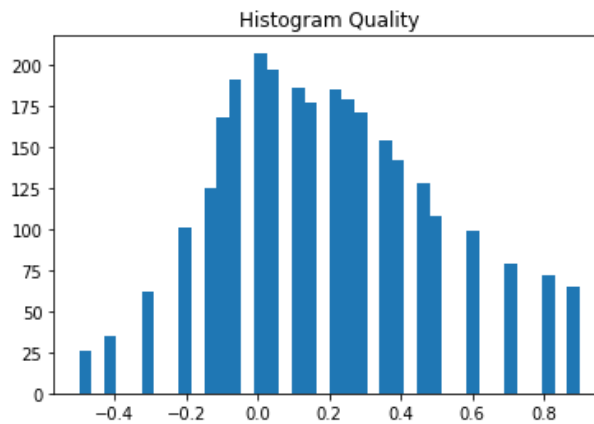
Figure 28. Distribution of the quality

It could be said that the quality distribution of the Figure 28 is binomial, since the distribution is discrete. This is because the database is formed in such a way that the quality does not take a continuous range of values, but the heat flux value has been calculated for certain values (it also occurs in the mass flux parameter and the pressure parameter). It has to do with the construction of the database, for the study of how different situations affect heat flux. Presumably, if the quality variable took more values among those selected (intermediate values), the distribution followed would be normal.

Hence, the groups are created considering if the flow is bubbly (low quality group) or annular pattern (high quality group) and a limit value (explained before) for patterns that are in between .Once the groups are created, the visual display through the boxplot is:
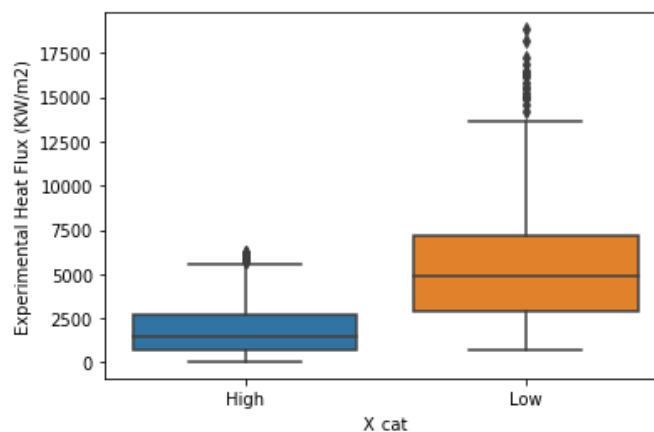
Figure 29. Boxplot of the heat flux for the two groups of quality

It is clear that most of the data in the high quality zone is equivalent to a lower heat flux than that of the low quality zone. This result is expected according to the heat transfer phenomena involved in

each flow pattern. In a high quality flow, the amount of steam is greater than the amount of liquid. The liquid has a much higher density than steam and a higher heat transfer coefficient, and that is why it is logical that, for a higher quality, the heat energy transfer in the critical heat flux is lower. Although it is vital to consider that boiling crisis and the decrease in the heat flux may happen for both (bubbly related to DNB, annular related to dryout). According to this, the ANOVA test confirms the above:

Statistic = 1697.2502815	p-value = 1.40606e-291

It should also be noted that, as explained above, to create the two quality regions, the Bubbly regime has been manually associated with the low quality, and the Annular regime with the high quality, and that also influences how the two groups affect the heat transfer. The complete analysis on quality is much more complicated than this, and it cannot be firmly stated that for a decrease in quality there is a decrease in the heat transfer coefficient. The phenomena that occur in the flow are complex and the interactions between the phases are beyond a simple description by means of a number associated with the quantity of each phase (such as quality or void fraction).

From here, the parameters of mass flux and pressure will be categorized to see their influence on heat flux and the subsequent analysis of the W-3 correlation.

2.4.2 Pressure categorical variable analysis

It is intended to evaluate the influence of pressure on the heat flow. In order to achieve this, two pressure groups are created, divided by the median of the total population. This categorization of the variable will also be useful to evaluate how different pressures affect the accuracy of the W-3 correlation. Hence the groups are created by a simple limit between the low region group and the high region group that is the value of the median.

The first thing to do is to evaluate the conditions of the pressure database and the groups performed. The pressure distribution function does not follow a normal distribution, so it will be necessary to apply a non-parametric test. In case the data samples are large, the assumption of normality of the data may be considered. In addition, the homogeneity of the variances is not satisfied either. Therefore, the test chosen to evaluate the two groups is the Welch test (non-parametric). To evaluate the homogeneity of the variances, the Levene test has been carried out, and the low p-value obtained denotes inequality of the variances.

Welch's t-test = -21.8894	p-value = 0.0000

Therefore, there are difference between the two pressure groups. The boxplot diagram:
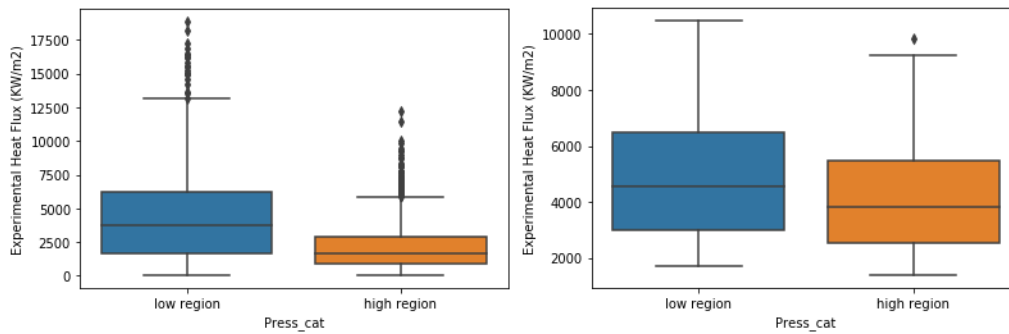
Figure 30. Boxplot of the heat flux for the two groups of pressure

The first plot corresponds to the unfiltered data and the second correspond to the filtered data for the W-3 correlation. The creation of two differently filtered databases corresponds to the need to meet with the requirements (the ranges established by the correlation). Apparently, not as many differences in the Heat flux values are observed for different pressures as they are observed for different qualities or flow regimes. But, as the statistical test ratifies, the differences exist (the tests have been performed for the two databases differently filtered and the conclusions were the same, although only the Welch test result was represented for the larger database).

2.4.3 Mass flux categorical variable analysis.

The creation of the groups to obtain a categorical variable has been made from the tertiles. The tertiles are values of the data that works as a boundaries to divide the data in three equal groups .In this way, three groups have been generated for the total mass flux group (low, middle, high). As before, the data for the total database and the filtered database for the correlation will be studied. Thus, in the first case, the associated p-value:

Statistic = 374.0298365	p-value = 6.03188356e-82

Considering the number of groups is three, it is necessary to observe for which groups a significant difference is observed:

```
=================================================================
   group1          group2     meandiff  p-adj   lower       upper    reject
-----------------------------------------------------------------
high region     low region  -2175.4037  0.001  -2447.485  -1903.3224   True
high region  medium region   -838.3708  0.001  -1131.5148  -545.2268   True
 low region  medium region   1337.0329  0.001   1041.532   1632.5338   True
-----------------------------------------------------------------
```

Table 9. Result of the Tukey test for the mass flux groups

The data shows that the difference exist for the three groups. This difference is showed as well in the boxplot:
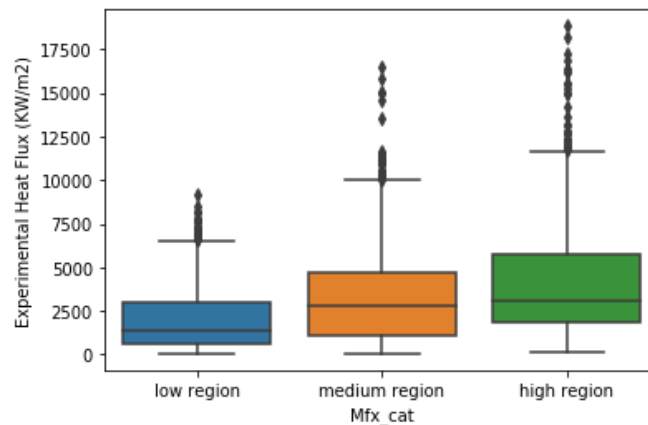
Figure 31. Boxplot of the heat flux for three groups of mass flux

Many values (of high heat transfer) are moving away from the natural trend in an unusual way, but it is not worrying considering the large size of the database. The diagram shows how high heat flux data tends to be more grouped in the high mass flux pool. The mass flux depends on the density of the flow (very low for gas compared to liquid) and therefore it makes sense to relate it to quality, which greatly affects heat transfer. The same is done for the database filtered for the correlation. In this case, the Levene test attracts attention since the p-value takes the following value:

Levene statistic = 0.46955149	p-value = 0.625680496659

Therefore, all samples taken have the same variance. To observe how the data is arranged this time, the box diagram is constructed again:
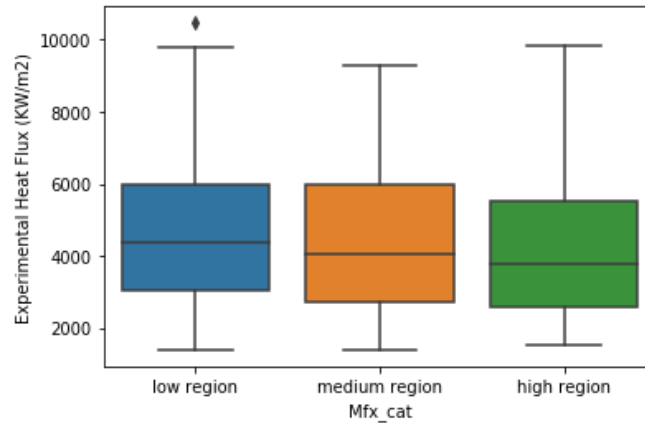
Figure 32.Boxplot of the heat flux for three groups of mass flux (data filtered for correlation)

Note that the range of the data is different because the data took this time is filtered to fit the W-3 Correlation range. Indeed, it seems that the differences between the two groups are not noticeable by simple visual observation. The result of the Kruskal-Wallis test for these groups (due to a non-normality distribution, this test must be used instead of the ANOVA test):

Statistic = 2.874769808	p-value = 0.237548158

The null hypothesis is valid since the value of the p-value is greater than 0.05, and therefore there are no differences between the groups. The three groups could be considered only one when calculating the heat flux. This result contrasts with the previous one that concluded that there are differences between the groups. This may be due to several reasons. To evaluate the relationship between heat flux and mass flux it is much more reliable to look at the analyzes performed on the entire database. Unlike this, for the database related to the correlation, some values have been thoroughly filtered so that the correlation can adequately predict the critical heat flux. This observation may lead to think that the W-3 correlation is somewhat sensitive to mass flow. To evaluate it, it can be compared the ratio between the measured and calculated flow with the mass flow and observe how it evolves. This comparison will be made later with the study of the correlation results.

Thus, it can be concluded that the levels of the mass flux do not affect the CHF in the given database, although there are no differences between the W-3 correlation data groups.

2.5   W-3 CHF Correlation analysis

The aim of this part of the work is to see how the Westinghouse W-3 correlation works, its results and see in what conditions fails more and in what conditions fails less. It is also intended to evaluate how they affect the different categorical variables created, especially the flow pattern variable.

To evaluate the correlation, the equation that has been implemented is the following:

$$q''_{crit} = F(X,p) * F(X,G) * F(D_e) * F(H_{in}) \qquad (46)$$

Which has been previously developed in the theoretical explanation of the correlation. When calculating the correlation, the term referring to the inlet enthalpy (F (H_{in})) and the form factor (F_s) have been neglected. The F factor (H_{in}) has been neglected because there is no data regarding the enthalpy inlet. Only information regarding local parameters at the CHF location are available in the database used, there is no information about the conditions at the inlet of the test section. Hence, it has not been used to calculate the correlation. Similarly, the factor Fs that refers to non-uniformly heated channels has been neglected since the database is created from uniform heat flux measurements.

The database chosen to analyze the correlation is the database filtered for the correlation itself; another database would not make sense. The units arranged in this correlation are British units.

To evaluate the accuracy of the correlation, a new variable is created. A ratio that defines the error between the experimentally extracted measure and the prediction made by the correlation.

$$Ratio = \frac{Heat\ flux\ measured}{Heat\ flux\ predicted} \qquad (47)$$

In case of perfect prediction, the ratio must have a value equal to one. Once the ratio is calculated, the distribution that follows this new variable should be a normal distribution, since a deviation from normality can be interpreted as systematic errors that have not been considered. The distribution of the ratio is as follows:

Figure 33. Histogram of the Ratio

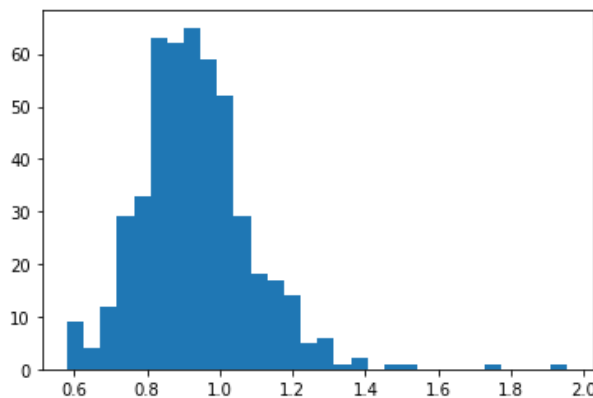The distribution follows a distribution similar to the normal (with some variations and atypical points dispersed). The mean and the median are slightly deviated from the unit:

Mean	Median	Standard deviation	Variance
0.9338176	0.920273	0.15697451	0.024640

Table 10. Parameters of the ratio data (filtered for the correlation)

The median and the mean have values lower than one, so the W-3 correlation tends generally to predict a higher heat flux than the heat flux observed experimentally.

Note*: Before continuing with the result obtained, it is interesting to apply the correlation to the complete database and see what the result is. The range of values is outside the range of application of the correlation, so it is expected to fail in the prediction of the critical heat flux. Looking at the histogram, there are values that are far away from the desired ratio (1).
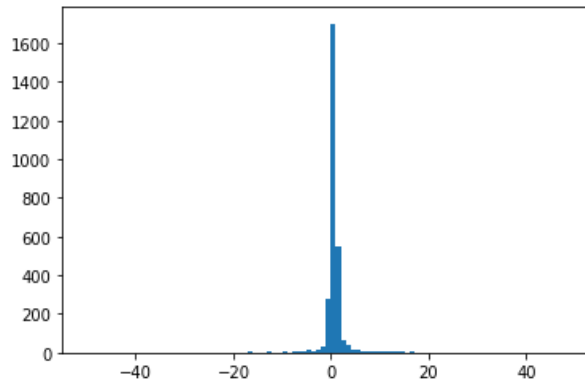
Figure 34. Histogram of the ratio (non-filtered data)

The histogram cannot even be interpreted since the deviation and the parameters are excessively deviated:

Mean	Median	Standard deviation	Variance
-2.0544833	0.79534210199	84.4451436	7130.9822900

Table 11. Parameters of the Ratio data for non-filtered data

Deviated values correspond to data that is outside the range of application of the correlation. In contrast, for the data group that is within the range, when the correlation adequately predicts the critical heat flux. That is why the median is close to the ratio one. The deviation of the data is inadmissible, in accordance to not having filtered the data for the W-3 correlation. *****

In order to observe graphically the deviation of the points, the experimental heat flux is plotted vs the predicted heat flux:
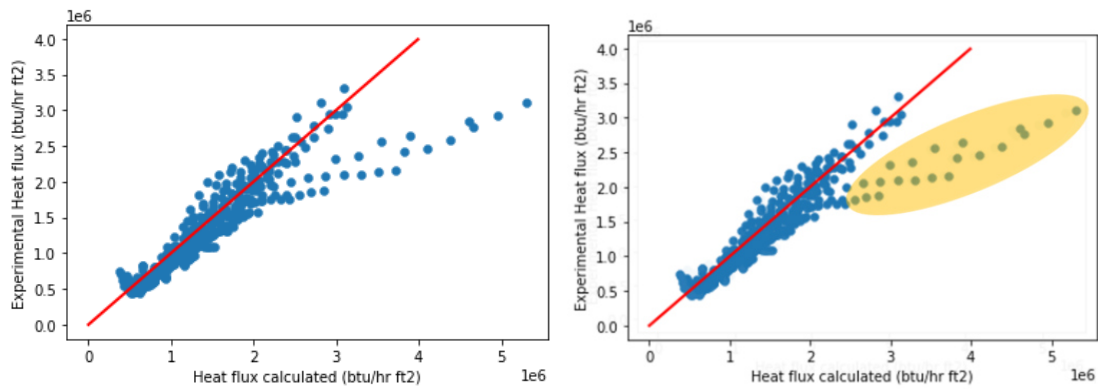
Figure 35. Experimental heat flux vs predicted heat flux by the correlation

The red line is a function of slope one that represents suitability when predicting heat flow. In general, the points follow a logical distribution around the perfect prediction line, but it can be seen a group of points that move away.

The following table represents the differences between the yellow zone values (error zone) and the total values:

|	Median all data	Median wrong ratio data	Mean all data	Mean wrong ratio data
Heat flux (BTU/hr ft^2)	1.28162e6	2.42472e6	1.40291e6	2.307980e6
Pressure (psia)	1740.452	2030.5283	1604.973	1991.851
Quality (-)	0.0	-0.4	-0.04656	-0.33999
Mass flux (lb/hr ft^2)	2.580681e6	4.055356e6	2.781389e6	4.104512e6

Table 12. Comparison of the parameters for the wrong ratio data and all the data (filtered for the correlation)

The difference of the parameters between the two groups of values is clear. The group in the error zone has, in general, a higher heat flux. Regarding the pressure, it can be observed how in the error group many data are accumulated near the limit of the correlation range (≈2300 psia). This may be an indicator of why this group of data fails more, because it is closer to the limits of performance of the correlation. Another point to note is that the correlation fails for some predicted points such as annular flow. Some data may not correspond exactly to DNB. Since the correlation is intended for the DNB type, it is normal that for these points, the heat flux is not predicted properly.

Most of the data is from the Bubbly regime. In fact, when representing only the Bubbly points, it is observed that the distribution is similar to that of the total database:
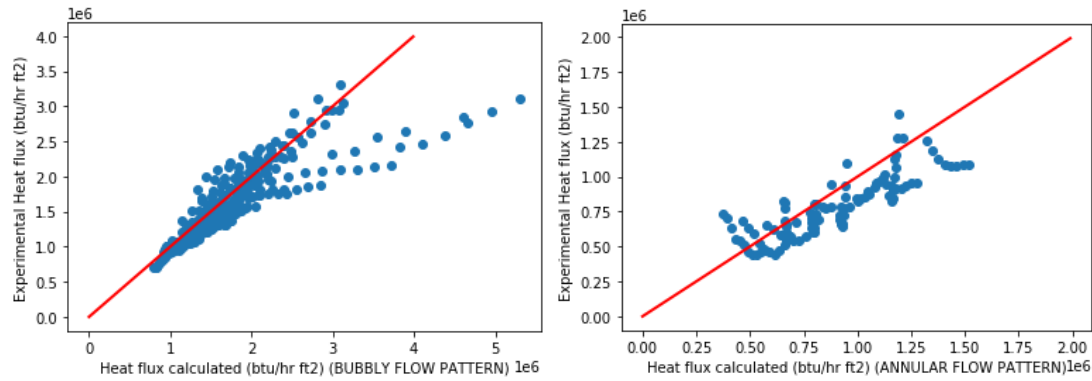
Figure 36. Experimental heat flux vs predicted heat flux by the correlation for Bubbly pattern (left) and Annular pattern (right)

Only the values that according to the Mishima method are annular flow are represented in the second graph. The distribution for the intermediate points follows a pattern in which the deviation of the data is uniform (the calculated heat flux is greater than the measured heat flux). As mentioned before, the W-3 correlation is only for critical heat flux of DNB type, and in principle for the Bubbly flow. However, the problem is that there is no methodology that ensures the exact prediction of the flow pattern. Since, in general, for the annular flow (according to Mishima) the predicted flow is higher than the measured one, a method that can be followed to improve the correlation (or a regression intended for the same purpose) is the application of a coefficient for this type of data. By adding a correct coefficient that only act for this type of data, the total correlation error could be reduced.

Regarding the distribution of the data for bubbly and for annular, the median of the Bubbly histogram is much closer to the unit ratio, even more than the total data set. The histogram of the annular data moves to the left where the ratio is less than the unit. It is logical because, despite the consideration made above, the closer to a flow with CHF of the DNB type, the better the correlation will work.

Likewise, the influence of the ratio for the other variables can be analyzed.

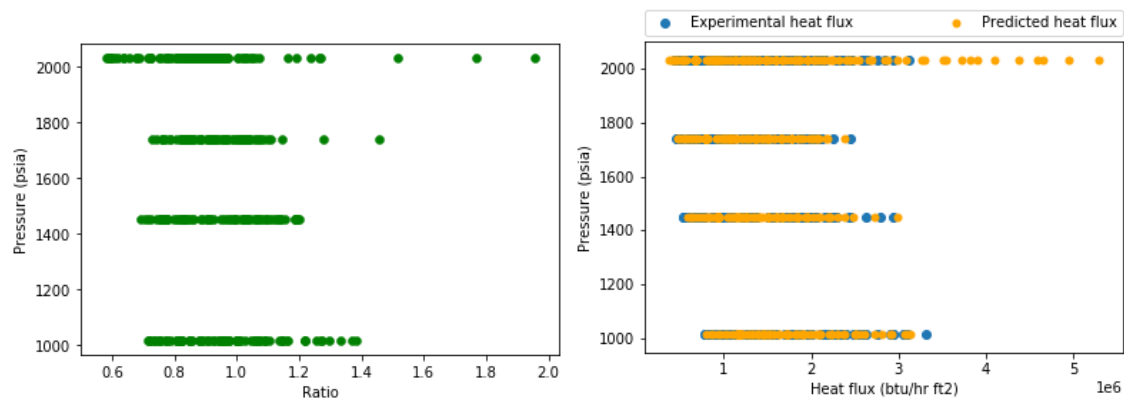## 2.5.1 Pressure

Pressure distribution vs the ratio:

Figure 37. Pressure distribution vs the ratio (left) and Pressure distribution vs Heat flux (both measured and predicted) (right)

In general, intermediate pressure data is closer to the ratio one. Similar conclusions have been drawn in the Table 12; the high pressure that is at the boundary of the application range provides very large errors. The categorical groups created in the section 2.4.2 for pressure can now be analyzed, but instead of analyzing the heat flux, the variable ratio (measured vs predicted) is analyzed. Three pressure groups (high, medium and low) have been created to evaluate the influence of the groups on the ratio. To assess this influence, several statistical tests are used:

Levene statistic = 1.2307	p-value = 0.29335

The three groups have the same variances, so the ANOVA test can be applied to see if there are significant differences between the groups, and, if there are differences, Tukey to see between which groups the differences exist.

ANOVA statistic = 5.98029	p-value = 0.0027968

```
=================================================================
    group1         group2      meandiff p-adj   lower   upper   reject
-----------------------------------------------------------------
high region      low region     0.0806 0.0028  0.0236 0.1377    True
high region  medium region      0.0502 0.0394  0.0019 0.0984    True
 low region  medium region     -0.0304 0.3802 -0.0843 0.0234   False
-----------------------------------------------------------------
```

Table 13. Results of the Tukey test for the pressure groups

The relevant differences in the ratio exist between the high pressure group and the other two groups. Hence, it can be concluded that in the high-pressure data (close to the application range) the greatest failures occur when predicting the CHF. This high pressure group takes different ratio values in comparison of the rest of the pressure data, which is closer to the ideal ratio value.

2.5.2 Quality
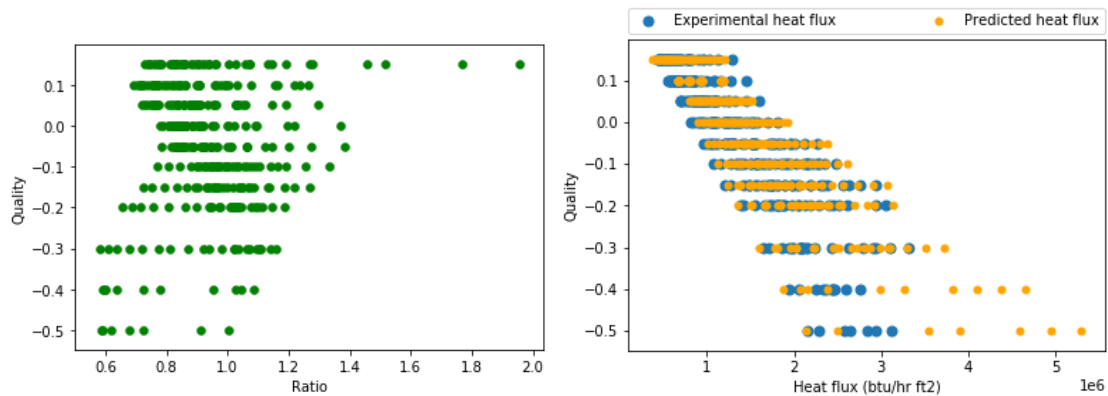
Quality distribution vs the ratio:

Figure 38. Quality distribution vs the ratio (left) and Quality distribution vs Heat flux (both measured and predicted) (right)

It can be seen in the plot the existing trend in the relationship between quality and flow. For a decrease in quality, the heat transfer coefficient also drops. This corresponds to the theory exposed in the introduction.

In the case of the relationship between the quality variable and the ratio, the influence is not clear. It is difficult to see significant patterns at a glance. Therefore, it is convenient to test the differences between the high and low quality groups for the variable ratio:

Leven statistic = 1.367417	p-value = 0.24305

ANOVA statistic = 3.726088	p-value = 0.05438335

The p-value of the ANOVA test shows that there are no significant differences in the ratio for different qualities (according to the proposed groups). Therefore, it can be concluded that the accuracy of the correlation is not sensitive to the change in quality (always considering the ranges established to achieve success in the prediction of heat flux of the correlation). It is true that the test result is at the limit of finding differences between the groups, but it must be taken into account that there are some different values that provide a large error in the prediction. It can be observed for example, for qualities at the upper limit of the range, and for very low qualities where the ratio also deviates a lot from the unit value. Note that while for the groups there may be no difference, some quality trend is visible, so something is missing. This is one of the drawbacks of creating categorical values, that it may be a loss of information.

2.5.3 Mass flux

Mass flux distribution vs ratio:
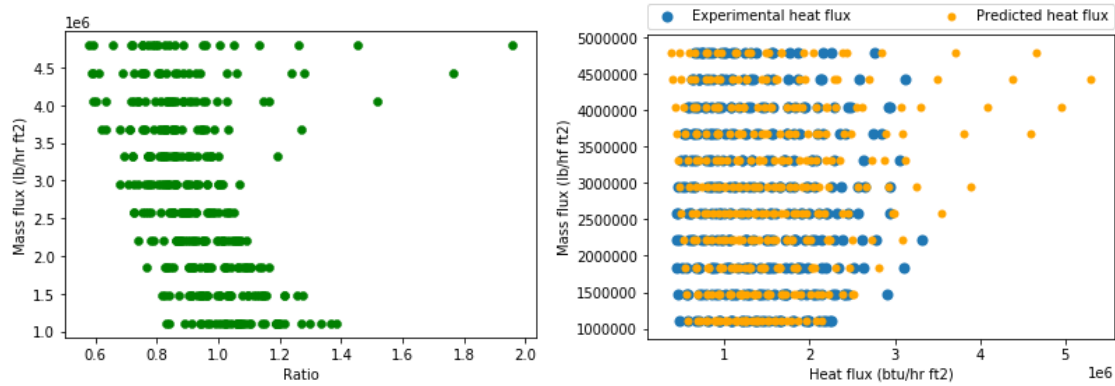
Figure 39. Mass flux distribution vs the ratio (left) and Mass flux distribution vs Heat flux (both measured and predicted) (right)

The correlation has better accuracy for medium ranges of the mass flow, which makes a lot of sense because the closer the mass flow gets to the range limits, the higher the error obtained. Especially it fails for high mass flow values. As can be seen in the histogram (Figure 40) of the high mass flow group, the ratios farthest from the unit are in this group, and the median value is deviated from the ideal value.
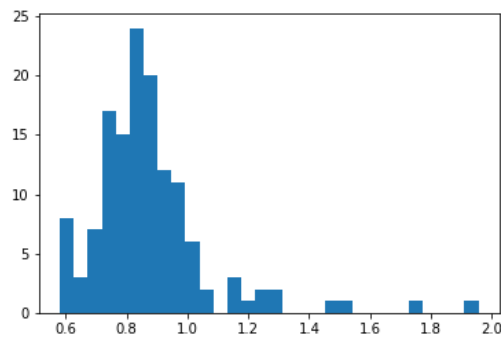
Figure 40. Histogram of the high mass flux group

After analyzing all the variables, one thing in common is observed: the accuracy of the correlation decreases when approaching to the limits of the range of use. An annotation to be made is that the parameters are in the formulation, so despite acting as a variable to analyze where the correlation fails, no visible trends should be found (if the formulation is correct):
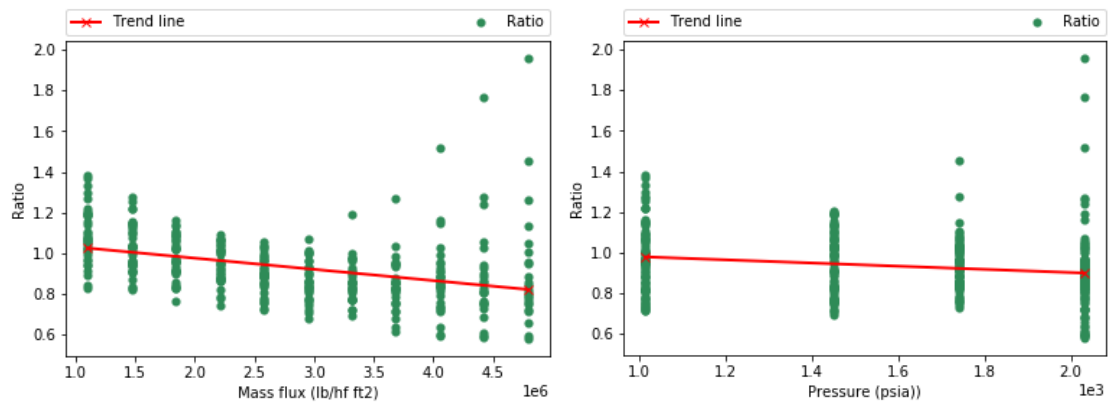
Figure 41. Ratio vs Mass flux with trend line (left), Ratio vs Pressure with trend line (right)
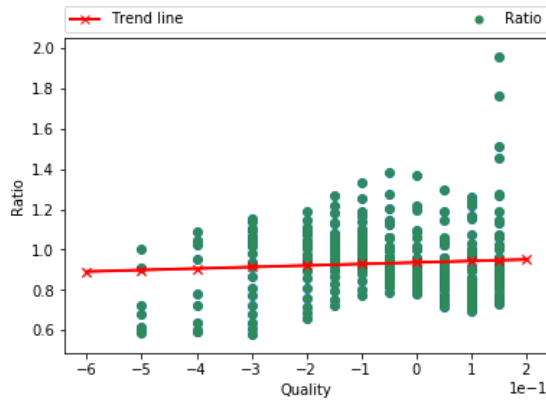
Figure 42. Ratio vs Quality with rend line

For the mass flux, there is a quite strong trend, for pressure is weaker, and in the case of the quality, the weakest. However, the existing trend is some nonlinear trend.

2.6 Regression

The objective of carrying out a regression is to try to predict the CHF from some input data, or, in any case, see if it is possible to do it. The possibility of predicting the flow of heat from a regression is doubtful, mainly due to the complexity of the physical phenomena that are present. It can be said that creating correlations is more complicated than carrying out statistical tests and estimating relationships between variables. In general, the reasoning performed to create correlations is to carry out statistical tests in order to know which variables are necessary to introduce in the correlation.

The regressions that have been carried out try to relate the input variables (pressure, quality and mass flux) to the CHF. The main idea is to check if different types of equations can compete with the W-3 correlation when preceding the CHF.

The groups of variables created can be used to improve the prediction of a certain regression. If we know how the CHF varies for certain groups of a variable, a binary variable can be introduced to adapt the prediction to more accurate values.

Before performing the regression, it is important to observe how related the variables are to each other. For this, the best tool available is a correlation matrix. From the coefficients, the relationship between variables can be quantitatively observed:

Figure 43. Correlation matrix of the Pressure, Mass flux, Quality and Heat flux

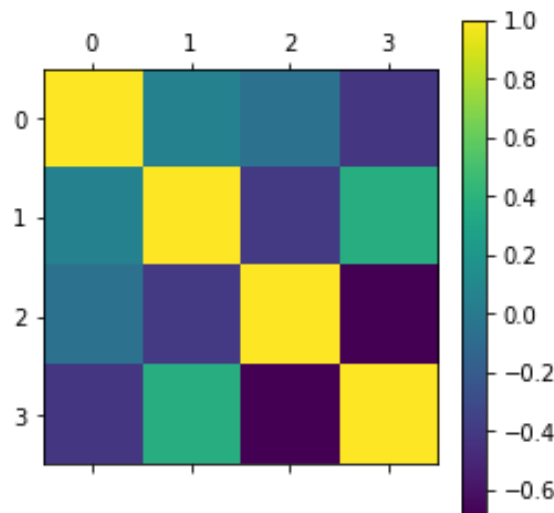The correlation matrix for the four variables. Each number represents the strength of the correlation as set out in the Table 14 (left). The variables in the correlation matrix are equivalent to the variables in Table 14 (right).

Coefficient	Correlation
1 – 0.8	Very strong
0.79 – 6	Strong
0.59 – 0.4	Moderate
0.39 – 0.2	Weak
0.19 – 0	Very Weak

0	Pressure
1	Mass flux
2	Quality
3	Heat flux

Table 14. Interpretation of the correlation matrix coefficients (left), labels of the parameters (right)

Negative values represent inverse correlations, where high values of one of the variables correspond to low values of the other. In the same way, a value of the coefficient equal to zero means that the two variables are not correlated.

In the matrix the first thing that is observed is the diagonal of value one, characteristic of all the correlation matrices. The heat flux variable is correlated, of course, with the rest of the variables. The greatest correlation exists between this variable and quality, with a strong correlation. For the two remaining variables (Mass flux and Pressure) the correlation with the heat flux is moderate. It can also be seen how the correlation between quality and heat flux is described by a negative coefficient, which makes sense, since at high quality values, heat flow generally decreases.

Regards the other variables there is no correlation (or there is a very low correlation), unlike the relationship between the quality variable and the mass flux variable. The correlation coefficient between these two variables is negative, and therefore describes that the higher the quality, the lower

the mass flow (in general). This coefficient makes sense since a high quality contains a large amount of vapor mass, which has a much lower density than the liquid phase. It is important to note that the analyzes extracted from the coefficients of the correlation matrix are extremely simple, and it is difficult to affirm something from a simple number. The relationships between variables are much more difficult to explain. Hence, the mass flux does not only depends on the quality but also of other parameters (although it is true that there is certain relation between quality and mass flux).

For a better global observation of the variables, the correlation matrix of the following type can be selected:
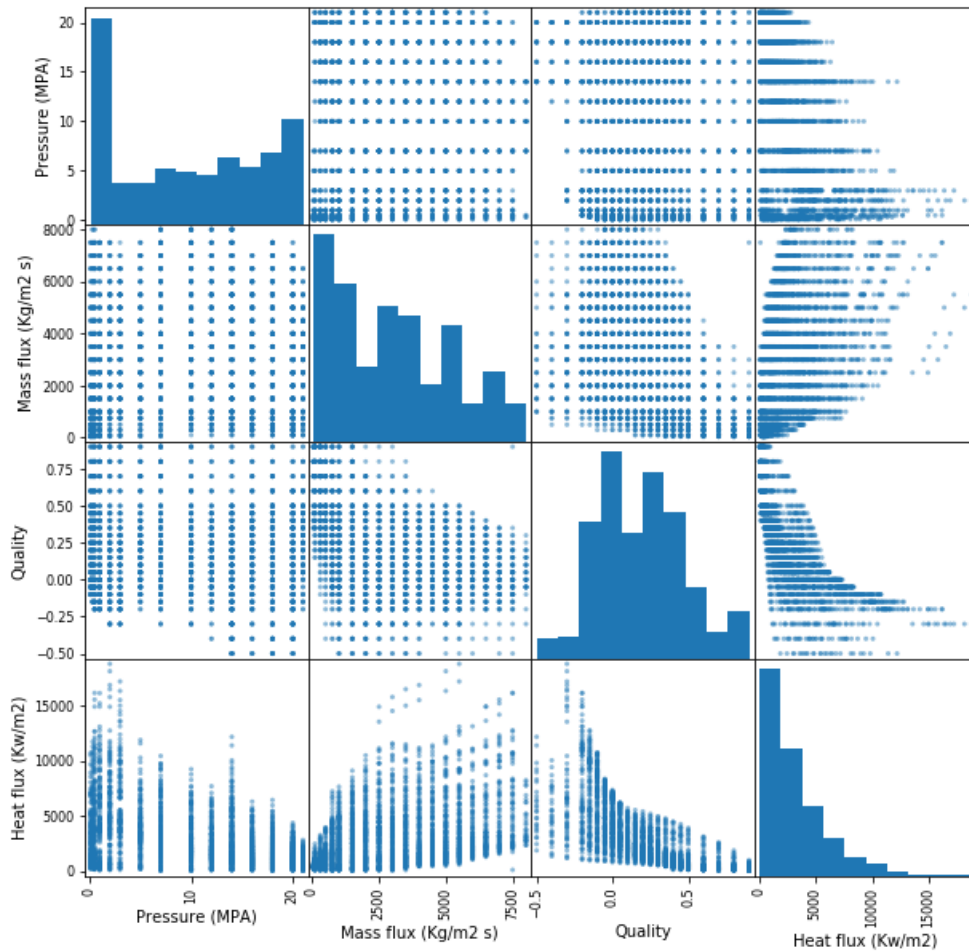
Figure 44. Correlation matrix with the plot of each variable of the data

In this correlation matrix (Figure 44), the total set of unfiltered data is plotted in order to visualize how the variables influence each other. In this matrix it is easily observable how each pair of variables evolves (one variable vs the other variable).

Two different methods have been used to carry out the regression and calculate the coefficients. In case the regression works properly, the two methods propose similar coefficients. The one method implemented is done through the sklearn library and the second method is done through the statsmodels library. The method is trained by means of the least squares method. Different regression models are proposed below.

2.6.1 First regression model

The first regression model proposed is the simplest, and proposes a prediction equation of the CHF of the form:

$$CHF(P, G, X) = ct + a_1 * X + a_2 * P + a_3 * G \qquad (48)$$

Parameter	Heat flux	Pressure	Mass flux	Quality
Units	btu/hr ft^2	psia	lb/hr ft^2	-

Table 15. Units used for the regression

This equation is the simplest to connect input variables with a variable to predict, since the relationship is linear. After carrying out the regression, the coefficients take the following values:

ct	2.192e+06
a$_1$ (quality coefficient)	-4.004e+06
a$_2$ (pressure coefficient)	-680.7385
a$_3$ (mass flux coefficient)	0.0420

Table 16. Coefficients calculated by the regression

From these coefficients, an equation capable of predicting heat flow is constructed. Now it is necessary to evaluate the accuracy of this new prediction equation by plotting the measured heat flux vs predicted heat flux, and the ratio.
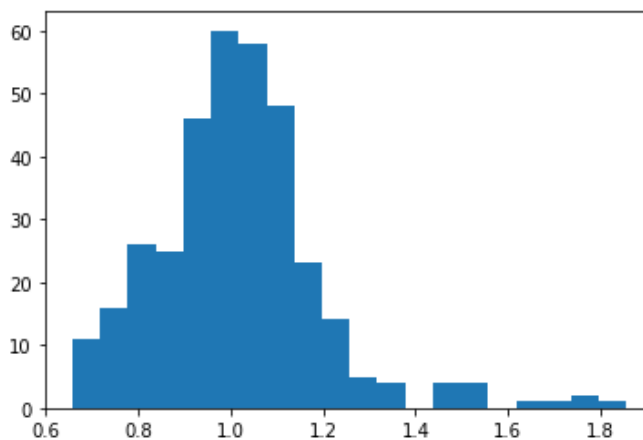

Figure 45. Histogram of the new predicted ratio of the first regression

The histogram distribution of the new ratio follows a look alike normal distribution although somewhat deformed. In addition, it can be seen atypical values for the ratio that reach values of almost two.
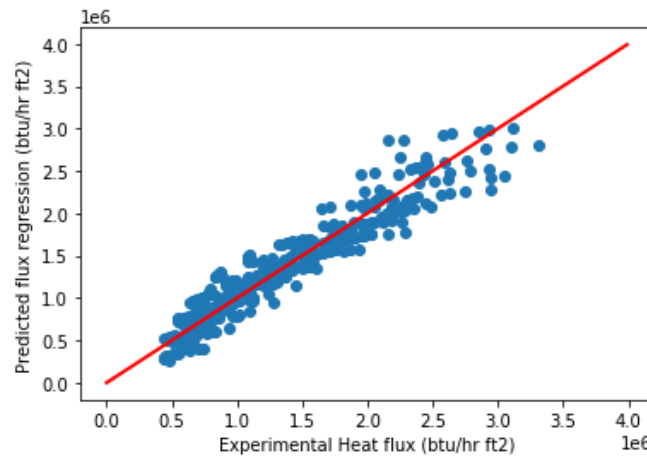
Figure 46. Experimental Heat flux vs Predicted Heat flux by the regression

In the Figure 46, it is observed how the first model of the proposed regression works. In order to analyze the success of the regression model, the mean squared regression error and the coefficient R^2 are displayed:

Mean squared error = 39610.41e6	R^2 = 0.903505

R^2 is a coefficient that determines the quality of the regression model to predict the results and their variations that can be explained by the model. The best possible value of the R^2 is the one, and the worst is the zero. A model that always predict the expected value of the predicted variable, disregarding the input variables, would get a R^2 coefficient of zero [16]. The results show that the regression works since the R^2 is close to the unit value. However, this model only accepts the same range of data that the W-3 correlation, so the comparison between the W-3 correlation and the first regression model is unavoidable. The parameters to check the success for the W-3 correlation are:

Mean squared error = 145133.96e6	R^2 = 0.64644151

The value of the W-3 coefficient R^2 is much lower compared to the regression coefficient. Therefore, it can be assumed that the regression works better to predict the CHF in that range of values. The lower dispersion is displayed in the plot:

Figure 47. Experimental Heat flux vs Predicted Heat flux for both the W-3 Correlation and the regression

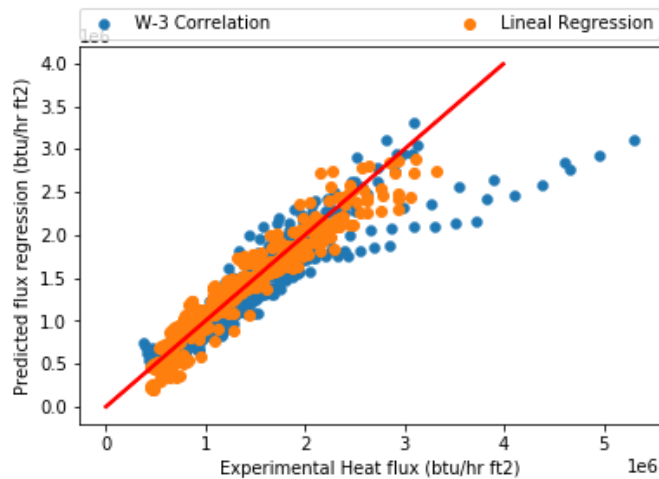However, a few considerations are important when reading the results. The fact that the regression works better for this group of data does not mean that the correlation is unfailingly worse. The regression is better for THIS group of data, and if another data (even similar) is used, it is better to perform a new regression in order to see if the creation of a new model to work with is possible. Furthermore, the relation expected by the model is linear, and the reality is way more complex than a simple lineal connection between the predicted variable and the input variable; and the Groeneveld database was created with measurements in pipes, which have significantly simple geometry than normal fuel assembly.

Now, it is possible to take profit of the categorical variables created in order to enhance the regression. The most important categorical value created is the flow pattern predicted (the others groups are created from already existing variables) and this variable is not implicitly included in the W-3 correlation. Hence, it is interesting to test this new created variable.

Since the variable is categorical (the variable flow pattern can only be equal to a string variable that assigns the type of flow (Bubbly, Slug, Churn, Annular…)), it is necessary a method in which including categorical values for the regression is possible. For this purpose, the method hot encoding should process the data in the column. One hot encoding is a process to convert the categorical variables in values that can be processed by the regression mechanism to improve the prediction. There are only three patterns present in the data, then the data can be disposed in two columns (Data = $2^{N^{\circ}binary}$) like this:

Encoding data one (e₁)	Encoding data two (e₂)	Flow pattern

1	0	Bubbly
0	1	Slug
1	1	Annular

Table 17. Hot encoding configuration to include the flow pattern categorical variable

This way, there are two new variables (e_1 and e_2) to include in the regression in order to improve the regression:

$$CHF(P, G, X, e_1, e_2) = ct + a_1 * X + a_2 * P + a_3 * G + a_4 * e_1 + a_5 * e_2 \qquad (49)$$

It is important to note that, for this new correlation, the coefficients a_1, a_2 and a_3 acquire new values:

ct	2.401e+06
a_1 (quality coefficient)	-3.573e+06
a_2 (pressure coefficient)	-682.4841
a_3 (mass flux coefficient)	0.0477
a_4 (encode one)	-1.346e+05
a_5 (encode two)	-2.053e+05

Table 18. Coefficients calculated by the regression (with hot encoding)

The parameters to test the accuracy of the new regression model are the following:

Mean squared error = 35195.34e6	R^2 = 0.9142611

It seems like the regression is a little bit better according to the new R^2 value. This method to include the influence of the pattern type is especially interesting when a specific error trend is found in a specific flow pattern. Thus, the error regarding that specific categorical variable (flow pattern in this case) can be reduced. The histogram follows a normal distribution

Once the regression considering the influence lineal has been tested, it is interesting to consider other types of influence between variables.

2.6.2 Second regression model

The second model proposed to perform the regression is the following:

$$CHF(P, G, X) = ct + a_1 * X + b_1 * X^2 + a_2 * P + b_2 * P^2 + a_3 * G + b_3 * G^2 \qquad (\,50)$$

The new model is able to consider relations between predicted heat flux and each variable in a different way ($y = ax^2$). Once the model is trained, the definitive coefficients

ct	2.446e+06
a_1 (quality coefficient)	-4.481e+06
a_2 (pressure coefficient)	-1047.6645
a_3 (mass flux coefficient)	0.0546
b_1 (quality quadratic coefficient)	-2.284e+06
b_2 (pressure quadratic coefficient)	0.1285
b_3 (mass flux quadratic coefficient)	-1.577e-09

Table 19. Coefficients calculated by the quadratic regression

With the following performing parameters:

Mean squared error = 34874.3090e6	R^2 = 0.91504326329

The coefficient R^2 is similar to the others but performing a lineal regression may not represent properly the behaviour.
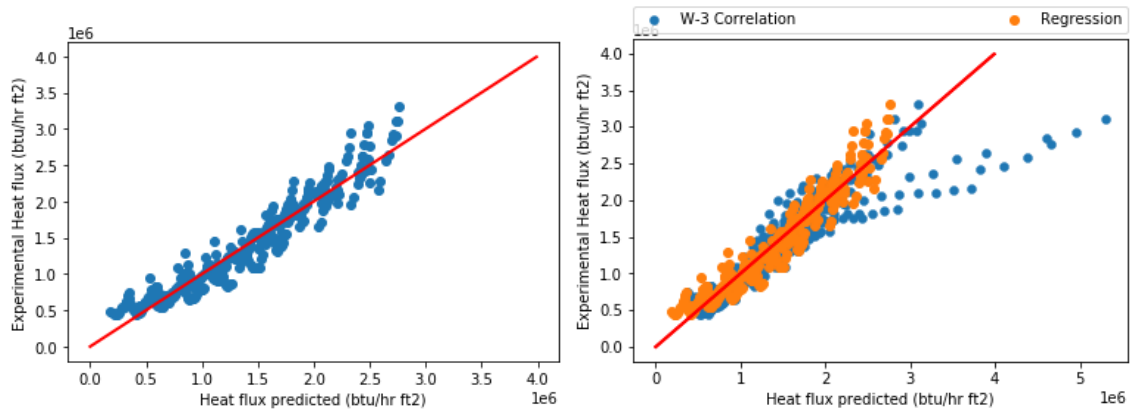
Figure 48. Experimental Heat flux vs Predicted Heat flux for both the W-3 Correlation and the second regression

The distribution of the second regression suffers a little change, but the performances are quite similar. In the Figure 48 (left), a wave shape trend is slightly appreciated. In the successfully regression models, the error is normally distributed and independent of predictors. So the measured versus predicted plot should look like randomly scattered points around the red line. If this does not happen, and a trend is visible, it seems that some trends are not captured by the correlation, and some variance is left. The error of this correlation is normally distributed but the trend appreciated at low heat flux predicted may indicate that the model is not taking into account some relation.

2.6.3 Third regression model

The equation proposed to predict the Critical Heat Flux is the following:

$$CHF(P, G, X) = ct + a_1 * X + b_1 * X^2 + a_2 * P + b_2 * P^2 + a_3 * G + b_3 * G^2 + c_1 * logP + c_2 * logG \qquad (51)$$

Note that the quality has not logarithmic form coefficient associated since the logarithm of zero does not exist. This equation pretends to implement the logarithmic relation that may exist between predicted and input. The prediction does not improve the results:

Mean squared error = 34821.0514e6	R^2 = 0.91517300

The change is not representative. Although there is no significant change (or even if the prediction is worse), it is important to check different possible relations. Observe that, in the ratio histogram, there are more points close to the unit compared to the histogram of the W-3 correlation, but in return, there are more atypical points with values way too far from the perfect prediction:

Figure 49. Histogram of the ratio for the Regression and the correlation (left), Experimental Heat flux vs Predicted Heat flux (right) for the third regression

Applying the hot encoding to include the flow pattern influence does not change too much the result either:

Mean squared error = 34224.1902e6	R^2 = 0. 91662700

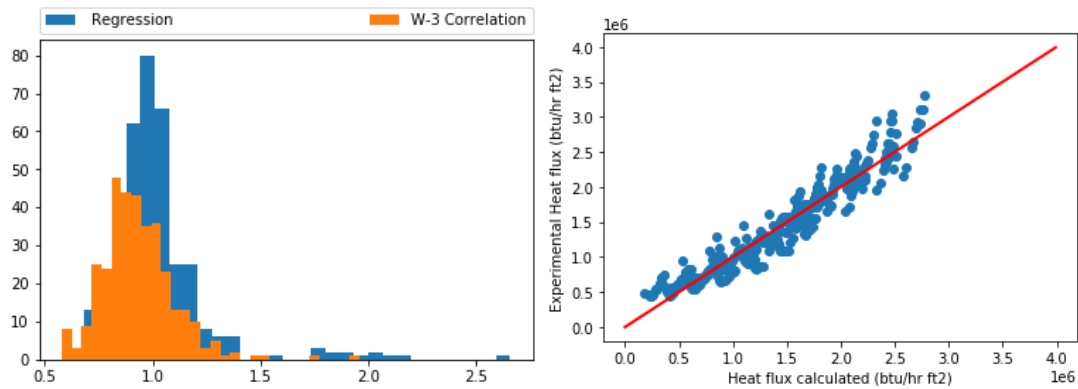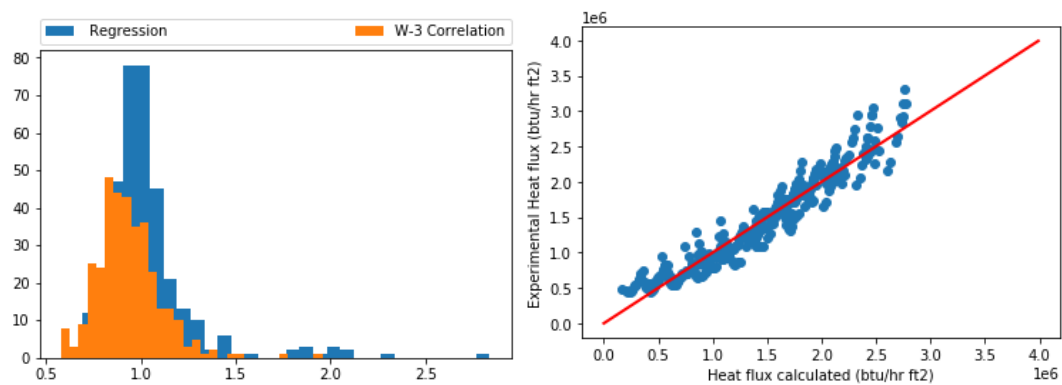In addition, the further plot of the results:

Figure 50. Histogram of the ratio for the Regression and the correlation (left), Experimental Heat flux vs Predicted Heat flux (right) for the third regression with the hot encoding

The results are similar in any case. Just a different peak of the histogram that represent a higher quantity of values close to the unit.

3. Conclusions

The conclusions extracted from the current work include different topics, all related somehow or other, to the Critical Heat Flux phenomena. Let this serve as a review and an introduction to understand the complexity in the accurate calculation of the CHF.

3.1 Critical Heat Flux review

The decrease in the efficiency of the heat transfer beyond the Critical Heat Flux value is key in the power generation industry, especially in the nuclear energy. It is no wonder that, since the first detection of the CHF, the creation and enhance of new models has been improving the current methods to predict the conditions of the phenomena. Considering the improvement in the energy production during the last decades, and the need to extract larger amounts of heat energy, the study of the CHF acquires crucial importance.

In the present work, it is underlined several times the high complexity of the physical phenomena of the CHF region. The heat transfer mechanisms vary depending on the pattern involved, and the determination of this pattern is not easy; sometimes it is even impossible achieve conformance. The existence of two phases with different behaviour, its distribution and its way of interaction are the reasons of this complexity.

The flow patterns try to describe the distribution of the phases, thus there is a manner to rate different types of flow. Through this classification, it is easier to find a way to explain which heat transfer methods are involved in a determined spectrum of conditions, defined by the pattern. Knowing the methods of heat transfer that happen in the flow (thanks to the understanding of the pattern that is going on), the prediction of the heat transfer and the parameters that affect is easier.

Therefore, it turns that the determination of the flow pattern is essential in the study of the CHF region. Not only the determination, but also analysis of each pattern to know accurately the heat transfer methods involved and the behaviour of the phases of the flow.

To conclude this section, it is important to emphasize in the difficulty of predicting the boiling crisis conditions, the CHF and the patterns. The challenge is such that there is no definitive model able to predict all the parameters with no condition constraint. The actual aim is to create models that allows engineers to work in terms of applicability and safety.

3.2 Prediction methods

The prediction methods are intended to calculate the heat transfer (specially the CHF in boiling crisis conditions) and/or the patterns involved to facilitate the labor. The most powerful codes to predict the CHF contain flow pattern prediction techniques to improve the preciseness. The main objective of the prediction methods is to achieve applicability and reliability. Many operate in reduced ranges that

ensure the success, and some others proceed in a wider range but at the expense of having procedures that are more difficult.

Some of these methods have been mentioned in the report but those analyzed in a deeper look are the Hewitt and Roberts map and the Regime transition criteria of Mishima and Ishii for the prediction of the flow pattern; and the W-3 Correlation for the prediction of the CHF.

Regarding the flow pattern predictors, the conclusions are very clear. The regime transition criteria developed by Mishima and Ishii [1] predicts properly the pattern. Although actually the only way to be sure of the pattern of the flow is by experimentation, the analysis of the variables of the data performed shows some interesting facts. The heat transfer theoretically changes with the patterns, and these variations should be noticed in the experimental heat flux of the flow. If the predictions done by the criteria were completely wrong, the aggregation of the data will display no interesting patterns of the evolution of the heat flux. However, the results show something very different. By grouping the data through the Mishima and Ishii criteria, the heat flux behaves (depending on the range of application and the conditions) as expected by the physical mechanism that happens in real conditions. The success of the method comes from the analysis of the physical mechanism of heat transfer and behaviour of the phases. The method is more complicated to apply than the maps for the flow pattern determination, and acts in a wider range. Compared to the map employed in the current work, the results are better. This is expectable since the Hewitt and Roberts map is older and much simpler. The map is more sensitive to changes in the range of application. Its objective is to provide a method to predict the pattern for a determined spectrum, so if the operation spectrum fits with the requirements, the map can act as an accurate prediction method. So that, the map of Hewitt and Roberts has not provide the results expected.

Regarding the CHF prediction, the method used is the W-3 Correlation. There are many correlations to provide a prediction of the critical heat flux, but since this correlation is simple and the fact that it was well documented and influential at the time of inception, it was chosen for the current work. What it has been seen is that the correlation work decent for the range of application, but still the range of application is not the only requirement for this correlation to work properly. The correlation is designed to work for DNB CHF type, and sometimes is hard to detect the pattern present in the flow. Hence, since it is hard to know when the departure from nucleate boiling may happen, it is also questionable when to use the correlation.

The purpose of this conclusion section is to highlight the importance of a good selection method to predict the heat flux and the occurring patterns. The present work provide the information to confirm the relevance of the predicting setting.

3.3 Correlations

During the work, the W-3 Correlation has been analyzed and compared with regression models of different type. The test are performed in order to give some relevant information about the accuracy of the correlation considering the operation conditions of the flow.

The test are performed for a data of different conditions, where the parameter of the heat flux is measured experimentally. With this data, the quality of the correlation and the regression has been tested through statistical coefficients. The results show that the regressions performed calculate the heat flux better. The atypical values of the correlation are closer to fit with the experimental measures, but for the bulk of the data, the ratio is calculated better (the histogram is way higher in the peak of values one). Does this fact mean that the correlation is essentially worse and the regression is always better? Not necessarily. Since the regression model is trained for a specific range of data, the regression may work properly for that specific data, but the regression does not consider the physical phenomena that happens, the relation of the phases, the behavior of the interphase, or other considerations that define the experimentally obtained critical heat flux. Perform a regression may be helpful when all the possible conditions and values are included in the training model, and then, with the proper test, it can serve as a fast way to get the variable that is needed.

In any case, the unique fact of performing a regression is valid in order to create a correlation. The way of creating a correlation is different. Performing a regression allows to visualize which factors should be include. By the observation of patterns in the data displayed, it is possible to know the type of relation between the input variable and the predicted one. It might be said that the regression model is a helpful tool to create a good correlation.

In this way, the data used to create the correlation is very important. The more data, the greater the accuracy and the possibility of finding relevant relations between the parameters involved in the phenomenon. For example, the Groeneveld tables are based on about fifteen thousand data, and this method predict the CHF better than the W-3 Correlation.

In conclusion, a combination of understanding of the phenomena and performing a regression should be enough to create a good correlation. This is not an easy task. Although the complexity of the phenomena prevent covering all the possible values, so the application of a determined range is generally required.

3.4   Regression and new correlations

As stated above, the creation of new correlations is not only made by performing a simple regression. Knowing the type relation between input variables and prediction variable is essential to create a prediction method.

Here, it may be interesting to create new "artificial" variables that help to enhance the accuracy of the prediction. "Artificial" because there are no defined parameters like pressure, temperature, density or quality, these variables refer to a state of the flow. They are referred to particular characteristics of the flow. Hence, a new variable can be introduced in the correlation to improve the prediction. Moreover, these new variables can represent, for example, the flow pattern. The new variables cannot

only represent marked patterns, but also specific behaviors that only occurs for determined conditions or range of operation. Thanks to this, a wider range of data can be predicted properly through the correlation.

During the current work, the use of hot encoding has allowed the introduction of the flow pattern in the model to predict the heat flux. The idea is to introduce coefficients that allow to include the changes in the heat transfer that happens when one flow pattern transits to another. Perhaps the way of including the coefficients is simple, but with a deeper study and bigger data, the success of the prediction may increase considerably (not only the success of the prediction but also the correlation may fit for a bigger range of conditions).

Including those coefficients introduces the need of calculating the flow pattern (in this case) but upgrades the model. Moreover, adding the prediction of the flow pattern in the correlation may build a full model to predict the Critical Heat Flux. This fact can be seen in different codes that cover all the features needed to make the most possible accurate prediction.

May the current project serve not only as an initiation in the CHF theory and its complexity but also as a way to understand the procedures that can be made to model the phenomena.

4. Bibliography

[1] Kaichiro, Mishima, and Mamoru Ishii. "Flow Regime Transition Criteria for Upward Two-Phase Flow in Vertical Tubes." *International Journal of Heat and Mass Transfer*, vol. 27, no. 5, Elsevier BV, May 1984, pp. 723–37. *Crossref*, doi:10.1016/0017-9310(84)90142-x.

[2] L S Tong, and Y S Tang. *Boiling Heat Transfer And Two-Phase Flow*. CRC Press, 1997.

[3] G. F. Hewitt. *Multiphase Flow in the Energy Industries*. June 2007.

[4] Hu, Hong, et al. "Boiling and Quenching Heat Transfer Advancement by Nanoscale Surface Modification." *Scientific Reports*, vol. 7, no. 1, Springer Science and Business Media LLC, July 2017. *Crossref*, doi:10.1038/s41598-017-06050-0.

[5] John G. Collier, and John R. Thome. *Convective Boiling and Condensation*. Clarendon Press, 1994.

[6] Noé Pinto del Corral. *Analysis of Two-Phase Flow Pattern Maps*. Brno University of Technology Faculty of Mechanical Engineering Energy Institute.

[7] G.Papathanassiou, et al. *Void Fraction Correlations in Two-Phase Horizontal Flow*. Los Alamos National Laboratory, 1983.

[8] Rouhani, S. Z., and E. Axelsson. "Calculation of Void Volume Fraction in the Subcooled and Quality Boiling Regions." *International Journal of Heat and Mass Transfer*, vol. 13, no. 2, Elsevier BV, Feb. 1970, pp. 383–93. *Crossref*, doi:10.1016/0017-9310(70)90114-6.

[9] Ruben Pompilio. *Experimental Analysis of Air-Water Two-Phase Flow in Vertical Large Pipes and Development of Drift-Flux Models*. Politecnico di Milano.

[10] S.G. Kandlikar. *Handbook of Phase Change*. Routledge, 2019.

[11] Song, Jin Ho, and Kyoo Hwan Bae. "Evaluation of Analytically Scaled Models of a Pressurized Water Reactor Using the RELAP5/MOD3 Computer Code." *Nuclear Engineering and Design*, vol. 199, no. 3, Elsevier BV, July 2000, pp. 215–25. *Crossref*, doi:10.1016/s0029-5493(00)00227-2.

[12] Soon Heung Chang, and Won-Pil Baek2. *UNDERSTANDING, PREDICTING, AND ENHANCING CRITICAL HEAT FLUX* . Oct. 2003.

[13] Stojan Petelin, and Bostjan Koncar. *PREDICTION OF VOID FRACTION IN SUBCOOLED FLOW BOILING*. Accessed 13 Feb. 2020.

[14] U.S. Nuclear Regulatory Commission. *RELAP5/MOD3 Code Manual*. Accessed 13 Feb. 2020.

[15] "A-to-Z Guide to Thermodynamics, Heat & Mass Transfer, and Fluids Engineering Online - Home." *A-to-Z Guide to Thermodynamics, Heat & Mass Transfer, and Fluids Engineering Online - Home*, http://www.thermopedia.com/.

[16] "SciPy — SciPy v1.4.1 Reference Guide." *Numpy and Scipy Documentation — Numpy and Scipy Documentation*, https://docs.scipy.org/doc/scipy/reference/index.html

[17] https://www.nuclear-power.net/sitemap-nuclear-power/.

[18] Thome, John & Cioncolini, Andrea. (2015). Two-Phase Flow Pattern Maps for Macrochannels. 10.1142/9789814623216_0019.

[19] Duarte, Juliana & Corradini, Michael. (2017). Hydraulic and Heated Equivalent Diameters Used in Heat Transfer Correlations. Nuclear Technology. 201. 1-4. 10.1080/00295450.2017.1389594.

[20] Mamoru Ishii. *One-Dimensional Drift-Flux Model and Constitutive Equations for Relative Motion between Phases in Various Two Phase Flow Regimes*. 1977.

[21] VDI Gesellschaft. VDI Heat Atlas. Springer Science & Business Media, 2010.

[22]Jacopo Buongiorno. NOTES ON TWO-PHASE FLOW, BOILING HEAT TRANSFER, AND BOILING CRISES IN PWRs AND BWRs. MIT Department of Nuclear Science and Engineering.

[23] "Regímenes y Correlaciones." Https://Poliformat.Upv.Es/Portal, Chemical and Nuclear Department (Universidad Politécnica de Valencia).

[24] Groeneveld, D. C., et al. "The 2006 CHF Look-up Table." Nuclear Engineering and Design, vol. 237, no. 15–17, Elsevier BV, Sept. 2007, pp. 1909–22. Crossref, doi:10.1016/j.nucengdes.2007.02.014.

[25] John H. McDonald, and University of Delaware. Handbook of Biological Statistics. 2009.